*People's Democratic Republic of Algeria*

*Ministry Of Higher Education And Scientific Research*

University Of Ghardaia

Faculty of Science and Technology

Department of Automatics and Electromechanics

N° d'ordre :
N° de série :

**A thesis submitted in fulfillment of the requirements for the degree of**

# MASTER

**Domain:** *Sciences and Technologies*

**Branch:** *Electrotechnics*

**Specialty:** *Renewable Energies on Electrotechnics*

# Theme

# Optimization of the parameters of a HIT heterojunction solar cell

**By :**

**Abdeldjalil BELLAKHDAR**

**Riyadh BELHADJ AISSA**

**Defended publicly on 03/06/2024**

**In front of the jury:**

| | | | |
|---|---|---|---|
| **Mohamed ARIF** | MAA | Univ. Ghardaïa | **President** |
| **Mohammed AZZAOUI** | MCB | Univ. Ghardaïa | **Examiner** |
| **Sifia BELGHERES** | MCA | Univ. Ghardaïa | **Examiner** |
| **Hadj Yahia SEBA** | MCA | Univ. Ghardaïa | **Supervisor** |

**Academic year 2023/2024**

## الملخص

يعد البحث عن مصادر الطاقة المتجددة أمرا حيويًا في مواجهة تراجع الوقود الأحفوري والمخاوف البيئية. وتتميز الطاقة الشمسية خاصة بفضل الخلايا الكهروضوئية بوفرتها ونظافتها ومع ذلك فإن تكاليف التصنيع المرتفعة تعيق اعتمادها على نطاق واسع. ولحل هذه المشكلة تهدف الابحاث إلى تحسين كفاءة التحويل مع تقليل النفقات. تعتبر الخلايا الكهروضوئية غير المتجانسة التي تجمع بين مواد مختلفة واعدة. تركز هذه الدراسة على تحسين خصائص الخلية مثل سماكة الطبقة الرقيقة وتركيز تطعيم اشباه النواقل في مختلف الوصلات المكونة للخلية باستخدام برنامج محاكاة $.AFORS-HET$

أظهرت النتائج أن طبقة الباعث الرقيقة والطبقات المتصة السميكة تؤدي الى تحسين الكفاءة.

**الكلمات المفتاحية :** وصلة غير متجانسة، الخلايا الكهروضوئية، الخلايا الشمسية السيليكون، السيليكون الغير متبلور، $a-Si:H$ ، $AFORS-HET$ .

## Résumé

La recherche de sources d'énergie renouvelables est vitale face au déclin des énergies fossiles et aux préoccupations environnementales. L'énergie solaire, notamment grâce aux cellules photovoltaïques, se caractérise par son abondance et sa propreté. Cependant, les coûts de fabrication élevés freinent leur adoption généralisée. Pour résoudre ce problème, les développements visent à améliorer l'efficacité de la conversion tout en réduisant les dépenses. Le photovoltaïque hétérogène, combinant différents matériaux, est prometteur. Cette étude se concentre sur l'optimisation de paramètres des cellules photi-voltaique tels que l'épaisseur de la couche et la concentration de dopage de semi conducteur dans les differentes joncyion qui compose la cellule à l'aide du logiciel de simulation $AFORS-HET$. Les résultats montrent que des films émetteurs minces et des couches absorbantes épaisses améliorent l'efficacité. **Mot-clés :** hétérojonction, cellules solaires en silicium, photovoltaïque, silicium amorphe hydrogéné, $a-Si:H$, $AFORS-HET$.

## Abstract

The search for renewable energy sources is vital in the face of the decline of fossil fuels and environmental concerns. Solar energy, particularly thanks to photovoltaic cells, is characterized by its abundance and cleanliness. However, high manufacturing costs hamper their widespread adoption. To solve this problem, developments aim to improve conversion efficiency while reducing expenses. Heterogeneous photovoltaics, combining different materials, are promising. This study focuses on the optimization of parameters such as layer thickness and doping concentration using $AFORS-HET$ simulation software. The results show that thin emitting films and thick absorber layers improve efficiency. The optimized structure achieves a remarkable efficiency of 24.97%. These results highlight the importance of precise parameter optimization to maximize the performance of heterogeneous photovoltaic solar cells.

**Key-words :** heterojunction, silicon solar cells, photovoltaic, hydrogenated amorphous silicon,

$a - Si : H, AFORS - HET.$

# Gratitude

Before any further development of this work, it seems appropriate to begin this anniversary with thanks to those who have taught us so much during this journey, and even to those who have been kind enough to make this journey a very profitable one. This work is certainly our signature, but it remains the result of an entire team, so it is the combined efforts of everyone that led to the results that I present here. It seems to us, as this study draws to a close, to express our gratitude and appreciation to all the people who contributed to it directly or indirectly.

We thank the members of the jury for agreeing to consider this thesis.

We also thank Mr. SEBA Haj Yahya, who trained and supported us throughout this experience with a lot of patience and education. Present but leaving a lot of freedom in the choices of in-depth studies while placing his trust in us. His skills and experience were a good guide for this work.

To our mothers for their patience and kindness.

To our parents for the effort they rigorously created in us.

To our family and friends who have always supported and encouraged us during these years.

We would like to express to all these people our gratitude for allowing us to carry out this work in the best conditions over the last few months.

# Contents

# List of Figures

# List of Tables

# List of Symbols

| | |
|---|---|
| $E$ | Energy. |
| $E(X)$ | Electic field . |
| $Eg$ | Width of the forbidden band (gap). |
| $\rho(x)$ | Density of electric charges. |
| $n, p$ | Concentration of electrons and holes respectively. |
| $n_0, p_0$ | Concentration of electrons and holes respectively at equilibrium respectively. |
| $j_n, j_p$ | Current density of electrons and holes respectively. |
| $Jph$ | Current density of photo generation. |
| $J$ | Cel output current density. |
| $Jsc$ | Short circuit current density. |
| $N_a, N_d$ | Concentration of acceptor atoms and ringing atoms respectively. |
| $\tau_n, \tau_p$ | Lifespan of electrons and all respectively. |
| $\mu_n, \mu_p$ | Mobility of electrons and holes respectively. |
| $D_n, D_p$ | Diffusion constant of electrons and holes respectively. |
| $L_n, L_p$ | Diffusion length of electrons and holes respectively. |
| $L_c$ | Effective collection length.. |
| $U_n, U_p$ | Recombination rates of electrons and holes respectively. |
| $T$ | Cell temperature . |
| $Q$ | Quality factor. |
| $n_i$ | Intrinsic focus. |
| $S_n, S_p$ | Recombination speed of electrons and all on the surface respectively. |
| $\epsilon, \epsilon_1, \epsilon_2$ | Permittivity, Semiconductor permittivity 1,2 respectively. |
| $R(\lambda)$ | Reflection coefficient. |
| $Rs$ | Series resistance. |
| $Rsh$ | Parallel resistance. |
| $q$ | Charge of the electron. |
| $U_t = KT/q$ | Thermodynamic potential. |
| $V_d$ | Diffusion potential. |
| $V$ | Cell output voltage. |
| $Vco$ | Open circuit voltage. |
| $FF$ | Fill factor. |
| $SR(\lambda)$ | Spectral response. |
| $Pm$ | Maximum power. |
| $\eta$ | Conversion yield. |

| | |
|---|---|
| $WP$ | Thickness of layer P. |
| $WI$ | Thickness of layer I. |
| $WN$ | Thickness of layer N. |
| $HIT$ | Heterojunction with lintrinsic Thin layer |
| $IBC$ | Interdigitated Back Contact |
| $PECVD$ | Plasma-Enhanced Chemical Vapor Deposition |
| $PERC$ | Passivated Emitter and Rear Cell |
| $PERL$ | Passivated Emitter Rear Locally Diffused |

# General Introduction

The search for renewable and non-polluting energy sources is one of the major technological challenges of the 21st century, given the gradual depletion of fossil fuel reserves, the growing environmental issues associated with their use, and the increasing costs of extraction. The solution to these problems lies in harnessing renewable energies, with solar energy conversion through photovoltaics taking a prominent role due to its inexhaustible and clean nature. This energy conversion involves the direct transformation of solar energy into electrical energy, primarily facilitated by silicon solar cells, whose manufacturing processes are becoming increasingly efficient. However, the primary obstacle to the widespread adoption of this clean energy technology remains the high manufacturing costs compared to fossil fuels and nuclear energy. The challenge for the photovoltaic industry is to enhance the physical/economic efficiency ratio of solar cells by introducing technological innovations that improve conversion efficiency. This can be achieved by employing new materials and structures that boost photovoltaic performance while reducing manufacturing costs through simple and costeffective implementation techniques. Heterojunction photovoltaic cells are created by combining materials with different energy gaps. The silicon heterojunction involves contacting hydrogenated amorphous silicon (aSi:H) with crystalline silicon (c-Si), where the energy gap of a-Si:H is higher than that of cSi. Unlike traditional homojunction cells, the doped regions and surface passivation in heterojunction cells are achieved through a single deposition of hydrogenated amorphous silicon. This material offers excellent surface passivation qualities, and its electrical properties can be modified by incorporating doping impurities. In this context, we are focused on optimizing the parameters of various layers constituting a heterojunction photovoltaic cell through simulation using the AFORS-HET software. The cell is based on a crystalline silicon substrate with an emitter formed by amorphous silicon, both with and without an intrinsic amorphous silicon buffer layer. Our study is divided into three chapters. The first chapter, divided into three parts, first defines solar radiation. Then it reviews semiconductors and the P-N junction. Finally, it provides an overview of the basic operating principles of a photovoltaic cell and the structures of various silicon cells. The second chapter is dedicated to the study of heterojunction solar cells in general and the a-Si:H/c-Si heterojunction in particular. In the third chapter, we present our contribution, which involves a numerical simulation of the various parameters of the heterojunction solar cell [a-Si:H(n)/a-Si:H(i)/c-Si(p)], and the interpretation of the results obtained from the simulation using AFORS-HET software. We conclude this work with a general summary of the main results obtained and the future perspectives.

# Chapter I

# Generalities On Photovoltaic Solar Cells

# I Introduction

This chapter presents fundamental concepts essential to the field of photovoltaics. We'll start by exploring solar radiation. Then, we will look at semiconductors, the PN junction, photovoltaic conversion and the characteristics of solar cells. Finally, we will provide an overview of the various Structures of Silicon Photovoltaic Cells.

# II Solar radiation

Solar radiation,[1] energy emitted by the Sun, is electromagnetic in nature and varies from radio radiation to Gamma rays, with a main concentration in the visible spectrum around $0.55$ microns. At a distance of about $150$ million kilometers from Earth, the energy power of solar radiation outside the atmosphere is $1350\ W/m^2$, but this value decreases to about $1000\ W/m^2$ at surface level terrestrial due to atmospheric absorption.

- **Air mass (AM)**
  To evaluate the performance of solar cells, we use the concept of Air Mass (AM), which represents the ratio between the thickness of the atmosphere crossed by the direct radiation to reach the ground and the thickness crossed vertically of the location (see figure I.1). This number is calculated according to the equation: $AM = 1/cos\theta$, where $\theta$ corresponds to the angle formed by the Sun with its zenith. By convention, $AM0$ represents solar radiation outside the atmosphere, applicable in particular for space applications.

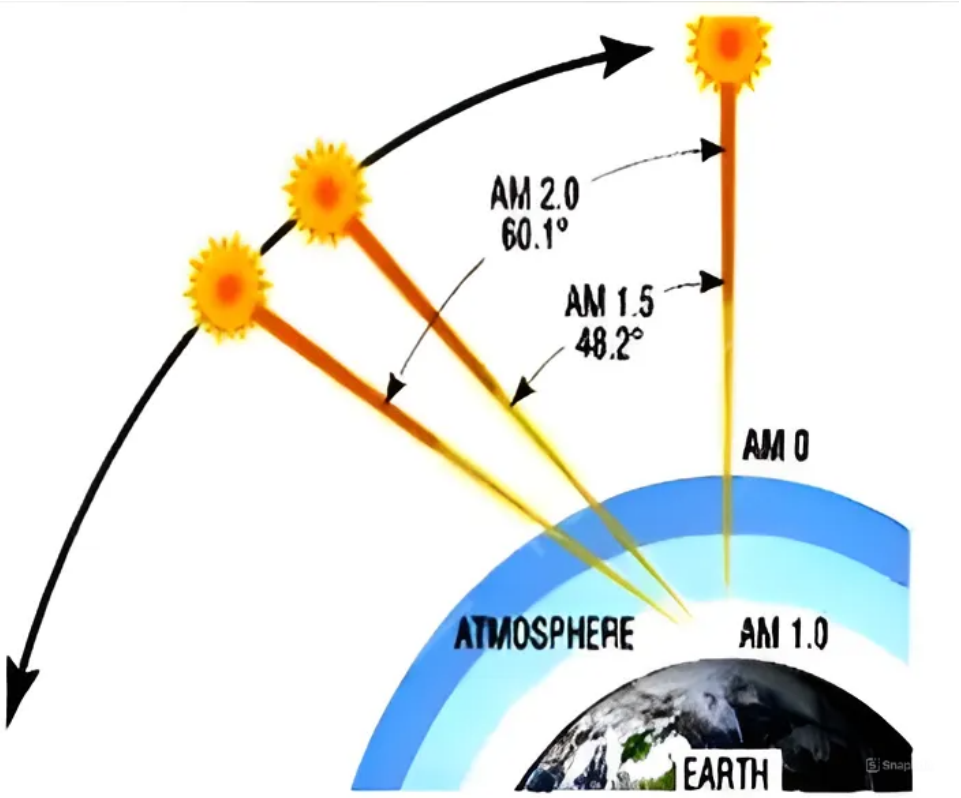


Figure I.1: Definition of air mass AMx.

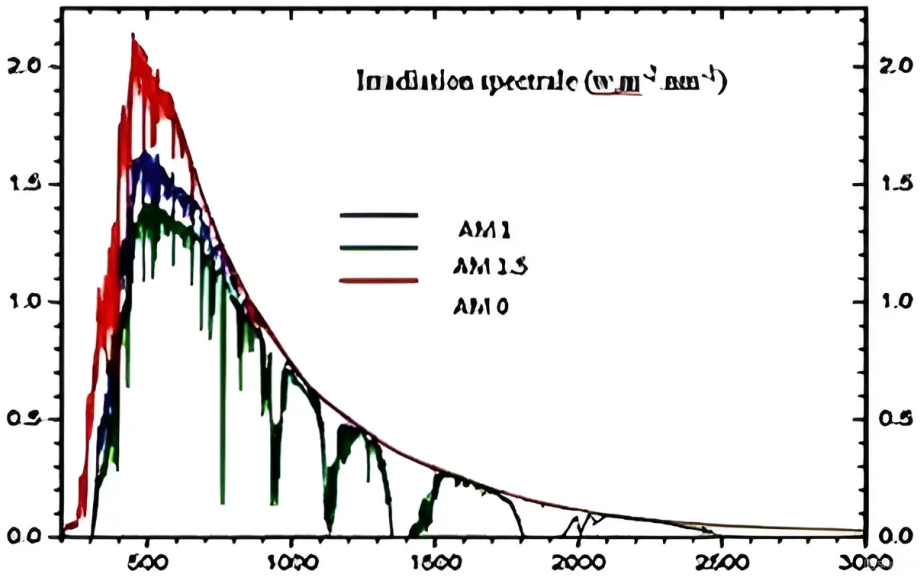


Figure I.2: Solar spectra recorded under several conditions according to the AM convention. (Source NREL solar spectrum).

- **Standard Test Conditions (STC)**

  To ensure a fair comparison of solar panel performance, rating standards have been established. These standards, known by the acronym STC (Standard Test Conditions), include

exposure to sunlight of $1000W/m^2$, an AM1.5 solar spectrum which implies an angle of incidence of sunlight of $48°$ (i.e. a ratio $1/cos\theta = 1.5$), and an ambient temperature of $25°C$.

# III Semiconductor

A semiconductor [4]is in an intermediate state between that of an insulator and a metal. At a temperature of $0\ K$, it behaves like an insulator, but its ability to conduct electricity increases with temperature, unlike metals whose conductivity decreases. Its band structure has similarities with that of insulators, including a narrow band gap which separates the valence band, completely filled, from the conduction band, the lowest of the permitted bands are empty at $0\ K$. When the temperature rises, thermal energy allows some electrons to move from the valence band to the conduction band, resulting in electrical conduction in the presence of an electric field. This conduction is due not only by electrons but also by holes, which are the locations left vacant by electrons in the valence band, adding an additional dimension to the conductive capacity of the semiconductor. Conductivity increases with the number of electrons present in the conduction band. This property of semiconductors, which allows their conductivity to be modified on a large scale, makes them particularly useful for the manufacture of active electronic components.

## III.1 Different types of doping

Pure, or intrinsic, semiconductors have limited utility on their own and instead serve as a basis for creating doped semiconductors by adding impurities, which changes their electrical properties. There are two main categories of extrinsic semiconductors:

- **N-type semiconductor**
  This type of semiconductor is characterized by a much higher concentration of electrons than that of holes, resulting from a larger quantity of electron donors compared to acceptors ($N_d - N_a > 0$). At room temperature, almost all donors are ionized. If Nd represents the concentration of donor atoms, the total density of free charge carriers (electrons) is given by the formula:

  $$n = n_0 + N_d \tag{I.1}$$

  Where $n_0$is the natural density of electrons resulting from the generation of electron-hole pairs by breaking covalent bonds.

- **P-type semiconductor**

  This semiconductor is distinguished by a concentration of holes significantly higher than that of electrons, due to a concentration of acceptors greater than that of donors ($N_a - N_d > 0$). Similar to the n-type semiconductor, the total density of holes in a p-type semiconductor is expressed by:

$$p = p_0 + N_a \tag{I.2}$$

  Where $p_0$ is the initial density of holes before doping.

## .1 Electro-optical properties

The electro-optical properties of semiconductors include several key phenomena:

- **Diffusion**

  In a semiconductor, in the absence of an electric field, the charge carriers (electrons or holes) move from an area of high concentration to an area of low concentration, this movement being driven by differences in concentration. This diffusion process is described by Fick's law, which establishes a relationship between the flow of charge carriers and their concentration gradient. The diffusion current densities for electrons and holes are, respectively:

$$\overrightarrow{I_n} = qD_n\overrightarrow{grad}(n) \tag{I.3}$$

$$\overrightarrow{I_p} = -qD_p\overrightarrow{grad}(p) \tag{I.4}$$

  $D_n$ and $D_p$ Are called the diffusion constants of electrons and holes, respectively. They are expressed in ($cm^2.s^{-1}$).

- **Recombination surface area**

  The surface area of a semiconductor plays a crucial role in its properties due to the irregularity of the crystal lattice and the incomplete chemical bonds of the atoms on the surface. On the surface, we find localized quantum states whose energy levels are often in the bandgap. These states can serve as effective centers of recombination, where an electron from the conduction band can move to a surface state and then recombine with a hole in the valence band. The probability of this process is greater than that of a direct passage of the electron from one band to another.

- **Surface recombination velocity (SRV):**

  SRV is an essential parameter for characterizing the surface properties of a semiconductor. It measures the rate at which excess charge carriers recombine via surface states and is mainly affected by surface imperfections and contamination. The surface cleaning can

significantly reduce SRV, sometimes by more than $100$ times, thereby improving semiconductor performance. The continuity of the current density at the boundary surfaces of the semiconductor material at the point $x = x_s$ (surface coordinate) is expressed by:

$$-qD_p \left(\frac{\partial p_n}{\partial X}\right)_{X=X_s} = qS_p \Delta p(X_s) = qS_p(p_n(X_s) - p_{n_0}) \tag{I.5}$$

For an N-type semiconductor and:

$$-qD_n \left(\frac{\partial p_p}{\partial X}\right)_{X=X_s} = qS_n \Delta n(X_s) = qS_n(n_p(X_s) - n_{p_0}) \tag{I.6}$$

For a P-type semiconductor. Where $S_p$ and $S_n$ are the surface recombination rates of holes and electrons respectively: The rate of electron recombination in a P-type semiconductor is:

$$U_n = \frac{n - n_0}{\tau_n} \tag{I.7}$$

And the hole recombination rate in an N-type semiconductor is:

$$U_p = \frac{p - p_0}{\tau_p} \tag{I.8}$$

The distance per run by a carrier over a lifetime is called the diffusion length, were

$$L_n = \sqrt{D_n \tau_n} \tag{I.9}$$

is the electron diffusion length; And

$$L_p = \sqrt{D_p \tau_p} \tag{I.10}$$

is that of holes.

## .1 PN junction

The PN junction is a fundamental component in the semiconductor universe, playing a crucial role both for its specific uses and for facilitating the understanding of the functionality of various other devices. This junction is formed with a semiconductor crystal in which the type and concentration of impurities vary depending on position, creating a transition from a P-type area to an N-type area. When these two zones come into contact, the excess electrons present in zone N migrate towards zone P. As a result, the part initially of type N acquires a positive charge, while that of type P becomes negative, generating thus an electric field which repels the electrons towards the N zone and the holes towards the P zone, forming what is called a PN

junction. The region where the charge is not neutral is known as the depletion zone. By placing metal contacts on the N and P parts, we obtain a diode.

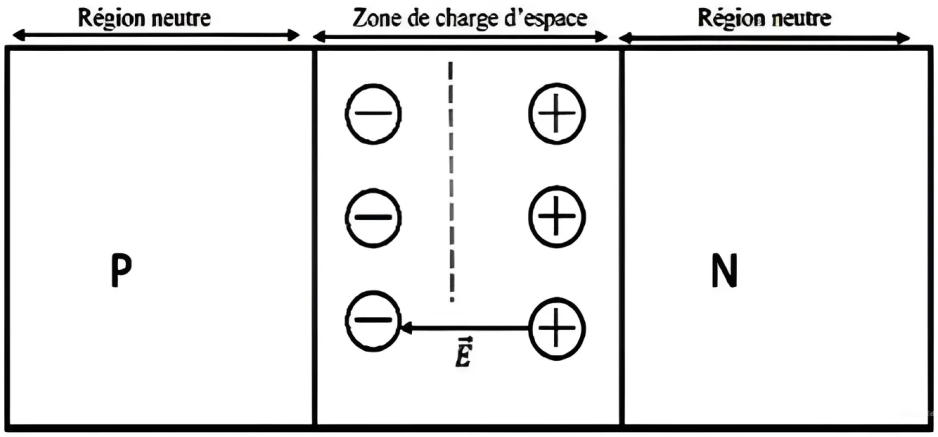


Figure I.3: Structure of the PN junction.

The PN junction configuration can be in two main forms:

- **Abrupt junction**
  It is characterized by a sharp and sudden transition in the concentration of impurities, remaining constant and positive in zone P, and constant but negative in zone N. The distribution of the doping impurities in the two regions P and N are uniform.

- **Gradual junction**
  This type of junction follows a linear variation in impurity concentration, where the difference between concentrations follows a linear relationship, indicated by $N_d - N_a = C_x$

Where $C_x$ is a positive constant, illustrating a gradual transition of impurity concentrations from zone P to zone N.

# I Solar cells

## I.1 Photovoltaic conversion

Photovoltaic energy[4]transformation involves three closely connected physical processes occurring at the same time:

- The capture of light by the material

- The transition from photon energy to electric charges;
- The accumulation of electrical charges.

Thus, it is essential that a material exhibits particular optical and electrical characteristics to facilitate the conversion of photovoltaic energy.

## I.2 Operating principle

The term "photovoltaic" derives from "phos", a Greek word meaning light, and the name of Alessandro Volta, [3]creator of the term "volt", referring to "electricity from light". This effect makes it possible to transform solar energy into electricity using a photovoltaic cell. This cell is made from a semiconductor material that transfers energy from photons to electrons, while an external circuit collects the created charge.

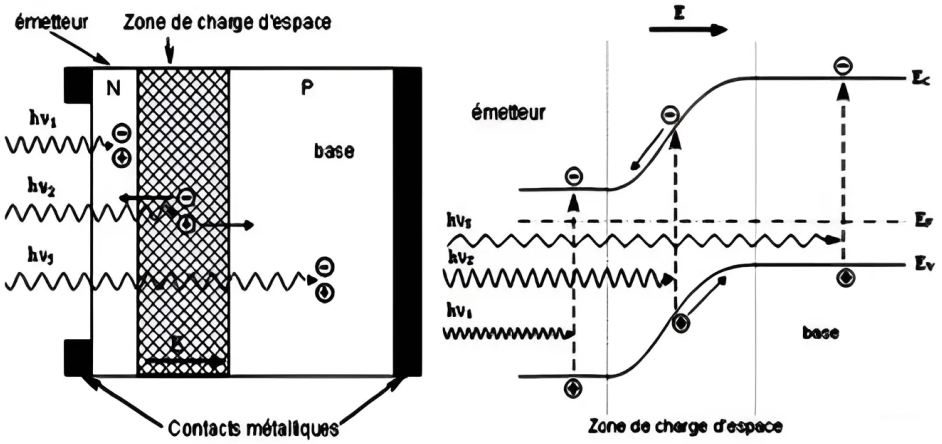


Figure I.4: Structure and band diagram of a photovoltaic cell.

When an incoming photon has an energy greater than the gap energy Eg (where $hv_0 > Eg$, or $v_0$ is the frequency of incident photon), it releases electrons from atomic attraction, making them pass from the valence band to the conduction band. This movement creates a free electron in the conduction band and a hole in the valence band, forming an electron-hole pair through the photoelectric effect, enhancing the conductivity of the semiconductor. The increased in mobility of electrons improves the conductivity of the semiconductor, but without orienting the charges by an electromotive force, they recombine, dissipating thermal energy without the possibility of conversion. The photoelectric effect near the contact surface between two p-type (excess positive charges or holes) and n-type (excess negative charges or electrons) semiconductors is crucial for directing the charge carriers. The joining of these p-type and n-type semiconductors creates a space charge zone (ZCE) or depletion zone, where diffusion leads to recombination

of electrons and holes, stabilizing the charges at the contact surface. This diffusion creates an internal electric field that prevents electrons from moving from n to p, effectively separating electron-hole pairs, with electrons predominating in the n zone and holes in the p zone. The ZCE functions like a diode, blocking the movement of majority carriers and facilitating that of minority carriers, thus making it possible to maintain charge separation. When an electron is released, it migrates from the p zone to the n zone, causing electrons from neighboring atoms to move to fill this gap. To simplify, this movement is associated with a "hole", a fictitious particle of positive charge moving in the opposite direction, from n towards p.

## I.3 Characteristics of a solar cell

The characteristics of a solar cell [2]are determined by its current-voltage (IV) curve, which clearly illustrates essential parameters such as cell efficiency, parasitic resistances, and fill factor. The current is evaluated as a function of the imposed voltage, both in the dark and under the effect of lighting. The presence of light causes the IV curve to shift downward into the fourth quadrant. This is due to the photoelectric current generated, which induces the production of energy.

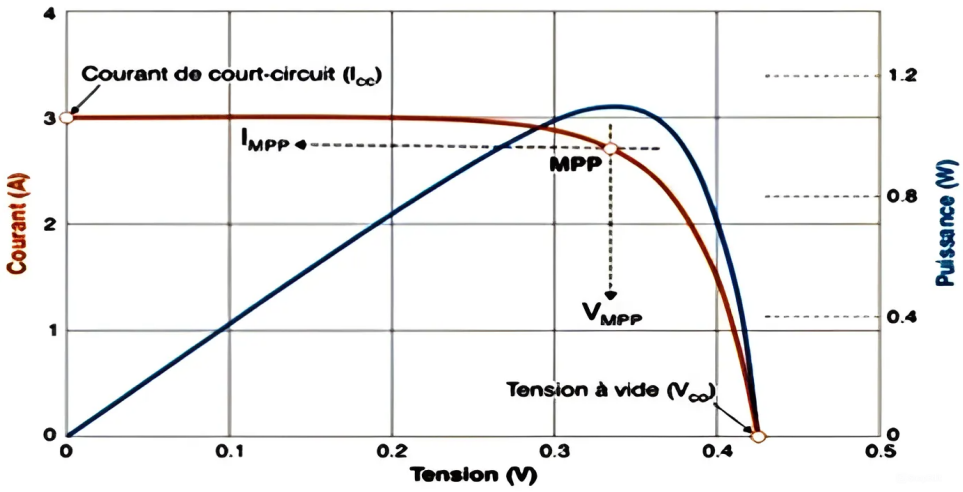


Figure I.5: I(V) characteristic of a photovoltaic cell.

### I.3.1 The short-circuit current Isc

The short-circuit current, denoted Isc, corresponds to the current flowing through a photovoltaic cell when it is short-circuited, that is to say when the positive and negative poles are connected together, making the voltage at the terminals of the cell equal to zero. In this situation, the

power produced by the cell calculated by $P = V \times I$ is also zero.

$$Icc = Iph/\left[1 + \left(\frac{Rs}{Rsh}\right)\right] \tag{I.11}$$

Or :
Iph: Photocurrent $[A]$, proportional to the irradiance F, with correction according to T.
Rs: Series resistance $[\Omega]$.
Rsh: Shunt (or parallel) resistance $[\Omega]$.

### .0.1 The open circuit voltage Vco

The open circuit voltage, denoted Voc, designates the voltage present at the terminals of a photovoltaic cell when it is in an open circuit state, i.e. when the positive and negative poles are electrically isolated from any other circuit, resulting in a zero current at through the cell. In this condition, the power delivered by the cell, expressed by $P = V \times I$, is equal to zero. Ideally, this voltage can be derived using the equation that describes the current-voltage curve of a photovoltaic cell by the expression:

$$Vco = \frac{kt}{q} ln\left[\frac{Icc}{I_0}\right] \tag{I.12}$$

With :
q: Charge of the electron $= 1.602.10^{-19}$ Coulomb.
k: Boltzmann constant $= 1.38.10^{-23} J/K$.
T: Effective temperature of the cell [Kelvin].
$I_0$: saturation current.

### .0.1 The fill factor FF

The fill factor FF is a crucial indicator of the quality of a solar cell. It is defined as the ratio between the maximum power that can be supplied by the cell and the product of the short-circuit current Icc by the open circuit voltage Voc, which corresponds to the maximum theoretical power if the cell ideally operated at these values of current and voltage.

$$FF = \frac{p_M}{Icc.Vco} \tag{I.13}$$

With :
$p_M$: maximum power.
This parameter, between 0 and 1, is expressed in % and describes the more or less rectangular shape of the IV characteristic of the solar cell.

### .0.1 The efficiency $\eta$

Conversion efficiency represents the percentage of incident solar light power that is converted into electrical energy by the photovoltaic cell. This efficiency is calculated by dividing the maximum power that the cell can generate by the power of the solar radiation received.

$$\eta = \frac{p_M}{E.S} \tag{I.14}$$

With :
$P_M$: Incident power.
If S is the surface area of the cell (in $m^2$) and E is the illuminance -irradiance- (in $W/m^2$). Or according to (I.3):

$$p_M = FF.Vco.Icc \tag{I.15}$$

$$\eta = \frac{FF.Vco.Icc}{E.S} \tag{I.16}$$

# I The structures of silicon photovoltaic cells

The majority of marketed solar cells, more than 90%, are made from silicon,[3] a semiconductor material benefiting from several advantages such as its terrestrial abundance and ease of extraction. Its extensive use in microelectronics has enabled the photovoltaic sector to acquire in-depth knowledge of this material and to master its technology. Crystalline silicon dominates the market, in particular thanks to its energy gap ideally suited to the solar spectrum.

## I.1 Standard structure of a silicon photovoltaic cell

At the heart of these cells is the pn junction, essential for the generation of electron-hole pairs and their separation before collection by electrical contacts. However, the initial efficiency of these cells is rather low, around 6%. To increase their efficiency, technologies have been developed to reduce recombination and improve photon absorption.

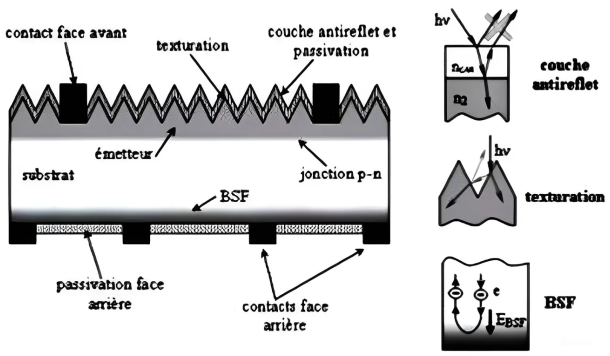


Figure I.6: Structure of a conventional solar cell with electrical contacts on both sides.

- **Anti-reflective layer**

  The reflectivity due to the high refractive index of silicon causes the loss of more than 30% of the sun's rays. To maximize photon absorption, an anti-reflective layer with a low refractive index is deposited on the silicon. This layer acts as a thin dielectric, creating destructive interference at certain wavelengths, particularly around 600 nm where photon flux is most intense. Solutions such as deposition of a double anti-reflective layer with different dielectrics are used to improve efficiency.

- **Texturization**

  In order to further reduce reflectivity, a surface texturization process is used, creating a micrometric relief which increases the absorption of photons by improving their penetration into the material. This method has achieved yields of up to 17%.

- **Passivation layer**

  Silicon substrates have a high density of structural defects, favouring the recombination of electron-hole pairs. To remedy this, a passivation layer, often made of silicon oxide or silicon nitride, is deposited to stabilize these defects.

- **Rear Surface Field (BSF)**

  To reduce recombination at the back surface, a back surface field is created by intensive doping, helping to keep minority carriers away from ohmic contact and minimize losses.

- **Front and Rear Contacts**

  The metal contacts, formed in a grid on the front face and covering the rear face, collect the charge carriers. Their design aims for a balance between reducing cell shadow and minimizing resistive losses, with a screen-printed front grille using primarily silver and an aluminium back layer.

## I.2 Advanced Structures of Silicon Photovoltaic Cells

- **PERC and PERL cells**

  PERC cells (Passivated Emitter and Rear Cell) and their improved version, PERL cells (Passivated Emitter Rear Locally Diffused), are distinguished by their ability to absorb a greater quantity of photons compared to standard cells. Standard cells are primarily limited to absorbing short wavelengths, while PERC cells, through passivation of their backside with a dielectric layer, can capture a wider spectrum of wavelengths, including those which would normally tend to pass through the substrate without being converted into electricity. This back layer also acts as a back surface field (BSF), preventing electrons from moving towards the back metallization and thus promoting their contribution to electricity generation.

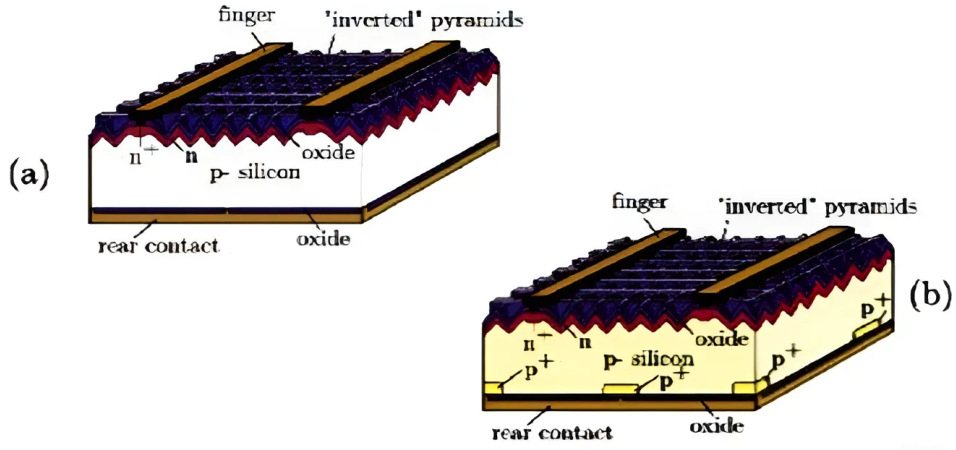


Figure I.7: Structure of PERC (a) and PERL (b) cells

In 1989, PERC cells reached an efficiency of 23.2%, thanks to passivation of both sides which reduces the recombination rate, allowing a higher open circuit voltage and better short circuit current density. PERL cells go further by diffusing boron only into the rear contact areas, creating a localized BSF layer that further reduces recombination while improving electrical contact, resulting in a significant improvement in form factor.

- **IBC cell**

  Introduced by Schwartz in 1975, the IBC (Interdigitated Back Contact) cell has high efficiency potential by placing all electrical contacts and junction at the back of the substrate. This configuration eliminates shading on the front face and allows the optical and electrical aspects of the cell to be optimized separately. These characteristics make IBC cells

particularly suitable for applications under high solar concentration.

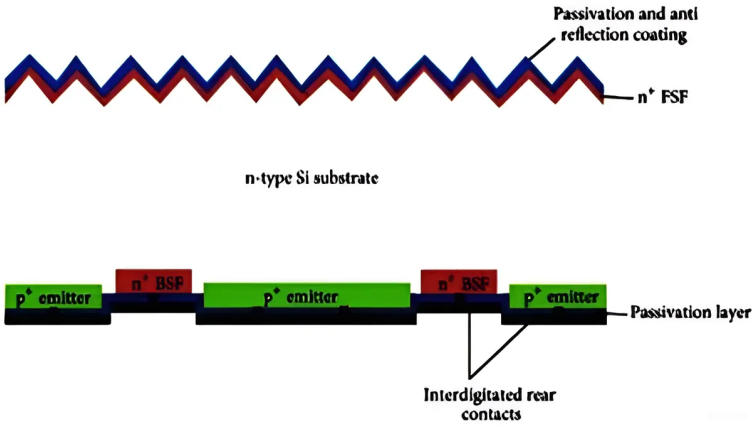


Figure I.8: Diagram of a cell with interdigitated contacts on the rear face (IBC).

- **Silicon Heterojunction (HET) Photovoltaic Cells**
  HET cells take advantage of a thin layer of hydrogenated amorphous silicon (a-Si:H) on the front surface to reduce the recombination rate by creating a heterojunction between two materials with different energy gaps. The presence of this layer makes it possible to generate a pn junction without requiring high temperature diffusion, which can preserve the integrity of the crystalline silicon substrate. These cells were initially explored for their electronic potential before being adapted for photovoltaic applications, resulting in promising initial efficiencies. In summary, developments in PERC, PERL, IBC, and HET technologies represent a significant evolution over standard cells, providing improved photon absorption, reduced recombination losses, and optimized charge collection. However, these technological advances involve more complex and potentially more expensive manufacturing processes.

# II Conclusion

In this chapter we highlight the technological advances in the field of silicon solar cells, emphasizing the importance of solar radiation as a source of renewable energy and different structures of silicon photovoltaic cells. It begins with an introduction to solar radiation, highlighting its electromagnetic nature and its influence on the production of solar energy on the Earth's surface. The study then delves deeper into the understanding of semiconductors, the P-N junction, and the photovoltaic conversion process, which are crucial to the operation of solar cells. Finally we see the different structures of silicon photovoltaic cells.

# Chapter II

# Photovoltaic Solar Cells With A-Si:H(n)/c-Si(p) Heterojunction

# I Introduction

The conversion of solar energy results from the absorption of photons, leading to the creation of electron-hole pairs. A permanent electric field within the structure allows for the rapid separation of these charge carriers to prevent recombination phenomena . In conventional solar cells, the electric field necessary for charge carrier separation is created by a PN junction typically formed by phosphorus diffusion on the same monocrystalline silicon substrate. However, the implementation of such cells entails high costs, although their efficiency is the highest. Hence, we find $A - Si : H(p)/c - Si(n)$ heterojunctions. This technology was introduced by the Japanese company Sanyo in the 1990 s and has achieved record efficiencies in cell and module production after several years . The initial cells were fabricated on structures where only the emitter is amorphous silicon (front heterojunction). The efficiency was around 18% [6], limited by the quality of the BSF. Subsequently, other structures were developed in which $A - Si : H$ is deposited on both the front and back sides of the substrate, thus creating two heterojunctions (double heterojunction). Efficiencies significantly improved to surpass 22% [7]. This technology enabled Sanyo to capture 8% of the global market share. This industrial success is attributed to the numerous advantages of the HIT structure . In this chapter, we will first introduce important concepts related to heterojunction solar cells. We will then study a-Si:H/c-Si heterojunction solar cells and their implementation in the photovoltaic domain. Finally, we conclude with criteria for optimizing silicon heterojunction cells.

# II Definition of Heterojunction

The term "heterojunction" refers to the junction between two semiconductors with different band gaps. If the two semiconductors are of the same type, the heterojunction is termed isotype, and if they are different, it is termed anisotype. It involves an epitaxial junction, meaning it is obtained by the direct growth of a semiconductor crystal on the surface lattice plane of another crystal. Such growth can only occur if the lattice constants of the two semiconductors are sufficiently close to avoid the presence of defects (such as dislocations) at the junction because epitaxy occurs at high temperatures. Figure (II.1) illustrates the emergence of a peak, which can also appear in the valence band depending on the nature and doping of the two semiconductors. The heterojunction aspect confers interesting properties due to the existence of band discontinuity. This structure has a larger active zone at the interface of the two semiconductors, and if the two materials absorb in complementary domains, absorption will be enhanced. The most important property is that a heterojunction can be used to control the position of free carriers by forcing them to reside and/or move in a welldefined confinement region. This is due to the

potential barriers that carriers will encounter, primarily the offset band gaps which are generally different for electrons and holes. The large interface of the heterojunction increases the number of excitons separated compared to a homo-junction structure. However, free charges created after the dissociation of the exciton are less likely to recombine since the geometry of the device itself leads to the spatial separation of electrons and holes, which migrate to the electrodes.

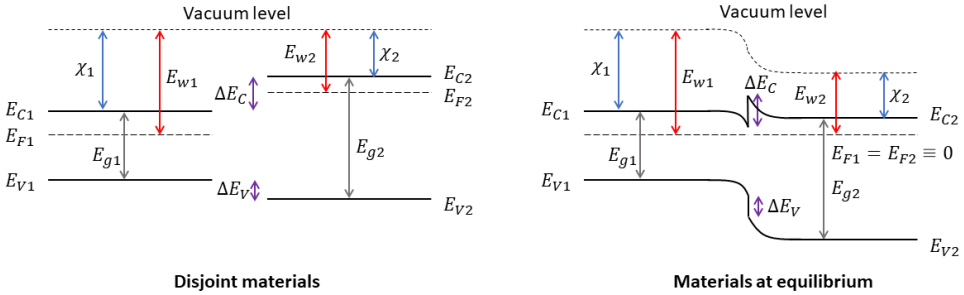


Figure II.1: Band diagram of an equilibrium heterojunction.

# III History of the first heterojunction solar cell

Walter Fuhs et al. were the first to conceive the idea of fabricating a-Si:H heterojunctions on c-Si as a component. Photovoltaic applications were not mentioned, but the concept of creating an a-Si:H/c-Si hetero-diode and its actual realization are credited to Walter Fuhs' team. In reference [8], the authors demonstrated the feasibility of depositing amorphous silicon on c-Si and obtaining a diode (rectifying effect, standard I(V) curve). The amorphous silicon (intrinsic) was evaporated (with a thickness of 1.5 $\mu$m) onto slightly doped p-type crystalline silicon. Sanyo was the first entity (laboratory or company) to successfully apply this idea to produce solar cells. The first publication dates back to 1991, with initial work from the late 1980s [9]. Sanyo used n-type c-Si, thus requiring p-doped a-Si:H to form a junction. The first implementation by Sanyo can be seen in Figure(II.3). TCO stands for Transparent Conductive Oxide.

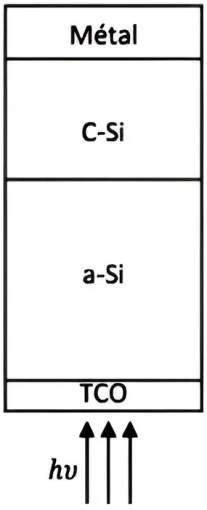


Figure II.2: Diagram of the first single heterojunction solar cell by Sanyo company.

With this new technology, Sanyo succeeded in capturing 5% of the market in 2002, and even 8% in a highly competitive market [10].

# IV The physical operation of a heterojunction

## IV.1 Heterojunction at thermodynamic equilibrium

Let's consider the heterojunction formed by bringing together two semi-conductors of different types and band gaps. Let's assume each of these two semi-conductor pieces is homogeneous . Let $N_a$ and $N_d$ be the concentrations of acceptors and donors in the p-type and n-type semi-conductors, respectively. When the two semi-conductors are brought into contact, electrons will diffuse from the n-type semi-conductor to the p-type one, and holes will diffuse in the opposite direction. This diffusion of charge carriers is a consequence of the very different concentrations of charge carriers in the two semi-conductors, resulting in an electric current of majority carriers called diffusion current . The electrons arriving from the p-side recombine with holes just after the junction. Thus, in a region near the junction, free holes disappear, leaving behind ionized acceptors (negative charges). Similarly, free electrons disappear from the n-side near the junction, leaving behind ionized donors (positive charges) . Ultimately, an area with uncompensated fixed charges (ionized impurities) is obtained around the junction. This area is called the depletion zone. Further from the junction, the semi-conductor retains its undisturbed properties and remains electrically neutral . An electric field appears, directed from

the + charges to the - charges, i.e., from the ntype semi-conductor to the p-type semi-conductor. Therefore, this electric field must be localized near the junction; it cannot exist in regions where there are free charges. As diffusion progresses, the electric field around the junction increases. Since it opposes the passage of holes from p to n and electrons from n to p, there is a decrease in the intensity of the diffusion current. A free electron that, following the generation of an electron-hole pair, arrives in the p-side near the junction (minority carrier) will be accelerated towards n by the electric field. Similarly, a hole arriving near the depletion zone in the n region will be accelerated towards the p region. This results in a minority carrier current (which adds to the majority carriers once they have crossed the junction), called drift current. This current flows in the opposite direction to the diffusion current . The drift current is relatively independent of the electric field at the interface. Indeed, it is limited by the generation of minority carriers and therefore reaches saturation value for relatively weak fields. At equilibrium, the electric field establishes a value such that the diffusion current is equal and opposite to the drift current.

## IV.2 Calculation of the electric field, potential, width of the depletion region (ZCE), and the differential capacitance

The determination of the potential distribution near the interface follows a similar approach to that of the PN homojunction, involving the integration of Poisson's equation. However, this process becomes notably intricate when dealing with space charge accumulation, mainly due to several factors. Primarily, the potential is contingent upon the charge distribution, yet given that these charges are free carriers, their dispersion relies on the potential itself. Consequently, achieving a self-consistent calculation without an analytical solution becomes imperative. Moreover, owing to the elevated carrier density within the accumulation layer, considerations for carrier correlations become essential. Lastly, since this charge accumulation occurs in close proximity to the interface, the image potential corresponding to these charges necessitates consideration. The analysis can be extended within the depletion regime, akin to the PN homojunction, where the depletion zone is devoid of free carriers. To establish a depletion space charge zone within each semi-conductor, they must exhibit differing types . Assuming homogeneous doping within the semi-conductors, we denote $N_{d_1}$ as the surplus of donors ($N_d - N_a$) in semi-conductor 1 and $N_{a_2}$ as the excess of acceptors ($N_a - N_d$) in semi-conductor 2[11]. The Poisson's equation is written as follows:

$$\frac{d^2v(x)}{dx^2} = -\frac{\rho(x)}{\epsilon} \tag{II.1}$$

In semiconductor 1 :

$$\rho(x) = qN_{d_1} \tag{II.2}$$

$$\frac{d^2v(x)}{dx^2} = -\frac{qN_{d_1}}{\epsilon_1} \tag{II.3}$$

By integrating once with the condition $E = 0$ at $x = x_1$, we obtain:

$$\frac{dv(x)}{dx} = \frac{qN_{d_1}}{\epsilon_1}(x - x_1) = E(x) \tag{II.4}$$

$$x = 0 :$$

$$E_{sc_1} = \frac{qN_{d_1}}{\epsilon_1}x_1 \tag{II.5}$$

By integrating a second time and denoting $v_1$ as the potential of the neutral region of semiconductor 1, we obtain:

$$v(x) = -q\frac{qN_{a_2}}{2\epsilon_2}(x - x_1)^2 + v_1 \tag{II.6}$$

In semi-conductor 2:

$$\rho(x) = -qN_{a_2} \tag{II.7}$$

$$\frac{d^2v(x)}{dx^2} = -\frac{qN_{a_2}}{\epsilon_2} \tag{II.8}$$

By integrating once with the condition $E = 0$ at $x = x_2$, we obtain:

$$E(x) = \frac{dv(x)}{dx} = \frac{qN_{a_2}}{\epsilon_2}(x - x_2) \tag{II.9}$$

$$E = 0 :$$

$$E_{cs_2} = \frac{qN_{a_2}}{\epsilon_2} \tag{II.10}$$

By integrating a second time and denoting $v_2$ as the potential of the neutral region of semiconductor 2, we obtain:

$$v(x) = \frac{qN_{a_2}}{2\epsilon_2}(x - x_2)^2 + v_2 \tag{II.11}$$

The electric field and potential are depicted in the following figure:

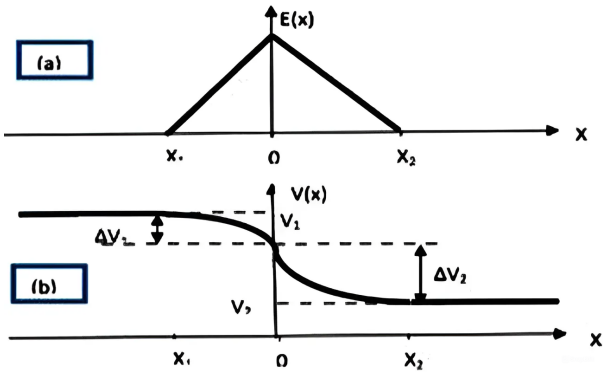


Figure II.3: Electric field and potential at the interface of a heterojunction $A - Si : H/c - Si$.

The continuity of the displacement vector at the interface is expressed as:

$$\epsilon_1 E_{s_1} = \epsilon_2 E_{s_2} \tag{II.12}$$

$$-qN_{d_1}x_1 = qN_{a_2}x_2 \tag{II.13}$$

The continuity of potential at $x = 0$ is written as:

$$\frac{-qN_{d_1}}{2\epsilon_1}x_1^2 + v_1 = \frac{qN_{a_2}}{2\epsilon_2}x_2^2 + v_2 \tag{II.14}$$

$$v_1 - v_2 = \frac{qN_{d_1}}{2\epsilon_1}x_1^2 + \frac{qN_{a_2}}{2\epsilon_2}x_2^2 \tag{II.15}$$

By setting:

$$w_1 = |x_1|$$

and

$$w_2 = |x_2|$$

We find:

$$N_{d_1}w_1 = N_{a_2}w_2$$

The relation (II.15) becomes as follows:

$$v_1 - v_2 = \frac{qN_{d_1}}{2\epsilon_1}w_1^2\left(\frac{\epsilon_1 N_{d_1} + \epsilon_2 N_{a_2}}{\epsilon_2 N_{a_2}} =\right) = \frac{qN_{a_2}}{2\epsilon_2}w_2^2\left(\frac{\epsilon_1 N_{a_2} + \epsilon_2 N_{a_2}}{\epsilon_2 N_{d_1}} =\right) \tag{II.16}$$

Hence the expressions for the width of the space charge zone in each of the semiconductors are:

$$w_1 = \left(\frac{2N_{a_2}\epsilon_1\epsilon_2}{qN_{a_2}(\epsilon_1 N_{d_1}\epsilon_2 N_{a_2})}\right)^{\frac{1}{2}}(v_1 - v_2)^{\frac{1}{2}} \tag{II.17}$$

$$w_2 = \left(\frac{2N_{d_2}\epsilon_1\epsilon_2}{qN_{a_2}(\epsilon_1 N_{d_1}\epsilon_2 N_{a_2})}\right)^{\frac{1}{2}}(v_1 - v_2)^{\frac{1}{2}} \tag{II.18}$$

The total width of the depletion zone is given by:

$$w = w_1 + w2$$

$$w_1 = \left(\frac{2\epsilon_1\epsilon_2(N_{d_1} - N_{a_2})^2}{qN_{d_1}N_{a_2}(\epsilon_1 N_{d_1}\epsilon_2 N_{a_2})}\right)^{\frac{1}{2}}(v_1 - v_2)^{\frac{1}{2}} \tag{II.19}$$

The potential difference $(v_1 - v_2)$ is established partly in each of the semiconductors. The ratio

of the corresponding potential drops is given by:

$$\frac{\Delta v_1}{\Delta v_2} = \frac{(v(x=0) - v_1)_{sc_1}}{(v(x=0) - v_2)_{sc_2}} = \frac{qN_{d_1}w_1^2/2\epsilon_1}{qN_{a_2}w_2^2/2\epsilon_2} = \frac{\epsilon_2 N_{d_1} w_1^2}{\epsilon_1 N_{a_2} w_2^2} \tag{II.20}$$

By using the relations (II.17) and (II.18):

$$\frac{\Delta v_1}{\Delta v_2} = \frac{\epsilon_2 N_{a_2}}{\epsilon_1 N_{d_1}} \tag{II.21}$$

In the absence of external bias, the potential difference $(v_1 - v_2)$ corresponds to the diffusion voltage. In the presence of a bias V applied to semiconductor 2 with respect to semiconductor 1, this difference becomes:

$$v_1 - v_2 = v_d - v$$

The diffusion voltage $v_d$ is distributed between the two semiconductors in the ratio:

$$\frac{\Delta v_{d_1}}{\Delta v_{d_2}} = \frac{\epsilon_2 N_{a_2}}{\epsilon_1 N_{d_1}} \tag{II.22}$$

As in the case of the PN homojunction or the Schottky diode, any variation in V leads to a modulation of the width W of the space charge zone and consequently a modulation of the charge developed in each of the semiconductors. As a result, the structure exhibits a differential capacitance. The space charge is given by:

$$Q_{sc_1} = -Q_{sc_2} = qN_{d_1}w_1 = qN_{a_2}w_2 \tag{II.23}$$

By specifying $w_1$ given by the expression (II.17) and $(v_1 - v_2)$ by $v_d - v$ we have:

$$Q = \left(\frac{2q\epsilon_1\epsilon_2 N_{d_1} N_{a_2}}{\epsilon_1 N_{d_1} + \epsilon_2 N_{a_2}}\right)^{\frac{1}{2}} (v_d - v) \tag{II.24}$$

The differential capacitance is given by:

$$c(v) = \left|\frac{dQ}{dv}\right| = \left(\frac{2q\epsilon_1\epsilon_2 N_{d_1} N_{a_2}}{2(\epsilon_1 N_{d_1} + \epsilon_2 N_{a_2})}\right)^{\frac{1}{2}} (v_d - v) \tag{II.25}$$

# I A-Si:H/ c-Si heterojunction solar cells

## I.1 Structure

Figure (II.4) illustrates a traditional heterojunction silicon cell where the contacts are located on both sides of the structure. On a crystalline silicon substrate, hydrogenated amorphous silicon (A-Si:H) layers are applied on both sides, forming heterojunctions with crystalline silicon. The A-Si:H layer on the front face, which is the face exposed to light, has a different doping than the c-Si substrate and is referred to as the emitter. On the backside, the A-Si:H layer, having the same type of doping as the substrate, is named BSF (Back Surface Field). A conductive and transparent oxide is then deposited above the transmitter, followed by the application of metal contacts on both sides of the cell.

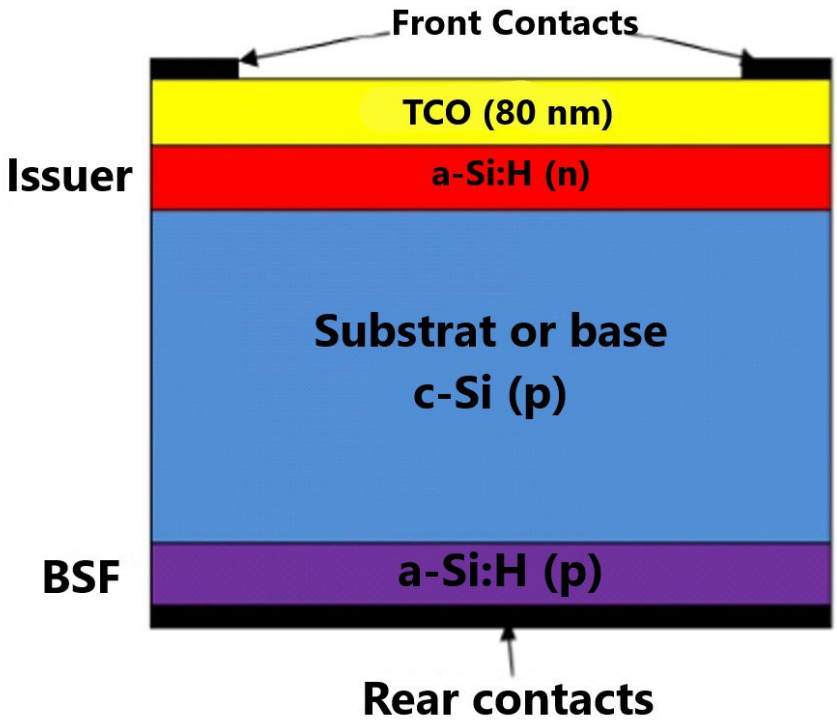


Figure II.4: A-Si:H/c-Si heterojunction photovoltaic cell structure.

## I.2 The two basic semiconductors: crystalline silicon and amorphous silicon

### I.2.1 Crystalline silicon

The selection of the optimal bandwidth gap for a solar cell is based on a compromise. A wider bandgap reduces saturation current (increasing Vco) but also decreases light absorption (reducing Jsc). The ideal bandwidth gap is estimated at 1.4 eV. The most efficient materials for photovoltaic applications are GaAs (1.42 eV to 300 K), InP (1.27 eV to 300 K) and crystalline silicon (1.12 eV to 300 K). Although silicon is not ideal, especially because it has an indirect bandgap limiting light absorption compared to direct bandgap materials like GaAs, it remains the most widely used material in the photovoltaic industry. In 2008, crystalline silicon cells accounted for 67% of the total photovoltaic module production market [12]. Crystalline silicon is prized for several reasons: it is abundant, non-toxic, easy to dope with boron or phosphorus, and benefits from the expertise of the microelectronics industry that uses very high quality and chemically stable silicon. Growth techniques to improve the purity of silicon, reducing defects such as dislocations, are constantly being perfected. There are several methods for making crystalline silicon:

- Monocrystalline silicon (c-Si) via the Float zone technique (Fz), producing materials with a load bearing life ranging from 500 $\mu$ s to 5 ms[13].
- Monocrystalline silicon produced by the Czochralski method (Cz), with a lifetime of load carriers between 50 $\mu$s and 500 $\mu$s .
- Multicrystalline silicon (mc-Si), which uses less refined materials and contains grain seals reducing load bearing life from 1 $\mu$s to 100 $\mu$s.

Monocrystalline silicon photovoltaic cells offer higher yields, but their production methods are more expensive. In contrast, multi-crystalline silicon is more economical, which explains its predominance in the photovoltaic industry.

### I.2.2 Amorphous silicon

The structure of amorphous silicon clearly differs from that of crystalline silicon, which presents a regular arrangement of atoms, by its random atomic lattice maintaining a local order at short distance. In the case of amorphous silicon, although the atoms maintain a regular distribution with their first neighbors (demonstrating a short-range order), the distances and angles of bonding begin to vary significantly as one moves away from a given atom, resulting in a long-range

disorder. This results in a random distribution of atomic positions and a rupture of many covalent bonds. Atoms in this disordered structure are characterized not by their specific position, but rather by the number of bonds they form with neighboring atoms, a notion of coordination introduced by Zachariasen in 1932. As shown in Figure (II.5) (b), in amorphous silicon, some bonds remain unsatisfied, while others are stabilized by hydrogen atoms.

The structure of amorphous silicon clearly differs from that of crystalline silicon, which presents a regular arrangement of atoms, by its random atomic lattice maintaining a local order at short distance. In the case of amorphous silicon, although the atoms maintain a regular distribution with their first neighbors (demonstrating a short-range order), the distances and angles of bonding begin to vary significantly as one moves away from a given atom, resulting in a long-range disorder. This results in a random distribution of atomic positions and a rupture of many covalent bonds. Atoms in this disordered structure are characterized not by their specific position, but rather by the number of bonds they form with neighboring atoms, a notion of coordination introduced by Zachariasen in 1932. As shown in Figure (II.5) (b), in amorphous silicon, some bonds remain unsatisfied, while others are stabilized by hydrogen atoms.

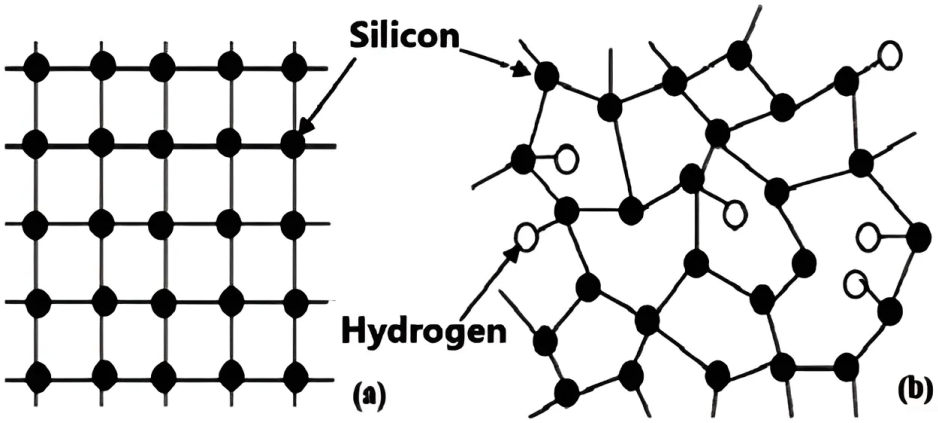


Figure II.5: Periodic networks (a) in crystalline silicon and (b) random networks in amorphous silicon. Silicon hydrogen.

In amorphous silicon, the random arrangement of atoms makes the traditional approach based on periodicity obsolete. However, Thorpe and Weaire's research in 1971 revealed that the presence of long-range order is not essential for the existence of a band gap in amorphous silicon: short-range order is sufficient for this [15]. Anderson's studies also highlighted the location of the electron's wave function due to the increase in disorder [16], revealing the existence of localized states either in the gap band or at the edge of the conduction or valence band.

## I.3 Components of the heterojunction silicon cell

### I.3.1 Conductive transparent oxide

In the standard configuration of a photovoltaic cell, a transparent conductive oxide (TCO) is applied to the front face, the illuminated face of the cell. To be effective, the TCO must have several key features:

- High optical transparency: Being placed on the front side, it is crucial that the TCO lets pass a maximum of light in order to promote the generation of electron-hole pairs.
- Good conductivity: This property is necessary to allow efficient collection of load carriers.
- Excellent adhesion: TCO must adhere securely to various types of substrates to ensure the durability and efficiency of the photovoltaic cell.

Conductive transparent oxides (TCO) are wideband materials that include a variety of oxides such as zinc, tin and indium oxides. The latter can be doped with various elements such as aluminum (Al), indium (In), gallium (Ga), fluorine (F) or tin (Sn). Tin-doped indium oxide, known as ITO (Indium Tin Oxide), is the most common and widely used TCO. The ITO is distinguished by its exceptional transparency, often exceeding 80% to 90% on the visible spectrum, a low resistivity ranging from $10^{-4}\Omega.cm$ to $5.10^{-4}\Omega.cm$ for the best samples, and up to $5.10^{-3}\Omega.cm$ for the least efficient. It also offers excellent adhesion on many substrates[17]. In the rear contact cells, the front TCO is replaced by materials that provide both the anti-reflective layer function and the surface passivation of the c-Si substrate, such as silicon nitride (SiNx), which is frequently used for this type of structure.

### I.3.2 The emitter

The emitter is formed of a thin layer of amorphous hydrogenated doping silicon opposite to that of the substrate, or of c-Si strongly doped in the case of a homojunction. This layer creates an essential p-n junction to separate the electron-hole pairs generated by light. It is crucial that this layer is very thin to reduce light absorption, while noting that it has a high square strength. This requires its coupling with an excellent conductor, whether it is metallic or a transparent conductive oxide, to efficiently collect the load carriers.

### I.3.3 The BSF

The BSF (Back Surface Field) is a layer that generates an electric field at the back and is also used to passivate the back of the cell. Composed of a strongly doped layer ($p+$ or $n+$), of the same type as that of the substrate, it creates a potential barrier thanks to the difference in doping level between the substrate and the BSF. This barrier helps to confine minority carriers in the substrate, preventing their recombination at the back of the cell. The BSF plays a crucial role in reducing back recombinations and improving the collection of majority carriers.

### I.3.4 Contacts

In standard solar cell structures, as illustrated in Figure (II.4), metal contacts are arranged on both sides of the cell. These contacts are essential for collecting the current generated by sunlight. Ohmic type contacts are ideal because they allow maximum current collection. For this, it is crucial to choose a metal that forms ohmic contacts and minimize contact resistance as much as possible. The metallization of the front face must balance the shading rate and the resistances in series. Reducing the shading rate increases the photogenerated current because more photons can enter the cell. However, this involves thinner metallizing fingers, which can increase the resistance in series. The main techniques for making metal contacts include:

- **Electrolysis:** This method is economical and offers good resistivity, but it requires several steps.
- **Evaporation:** It provides excellent resistivity and low contact resistance but is expensive and inefficient in terms of metal utilization performance.
- **Screen printing:** Economical and simple technique, suitable for high volume production, although developed at high temperature.

Screen printing is the most compatible technique with industrial standards and is increasingly preferred for its ability to realize fingers and buses of metallizations in a single step, in an economical and automatable way .

## I.4 Development and benefits of heterojunction silicon technology

The first components using a-Si:H/c-Si (diode) heterojunctions were developed by Walter FUHS team [18]. This innovation was commercially exploited by the Japanese company SANYO, which began its work on a-Si:H/c-Si heterojunction silicon cells in the late 1980s, with a first publication in 1991 [19]. SANYO is currently a market leader with its HIT (Heterojunction

with Intrinsic Thin film) cells, which integrate an intrinsic hydrogenated amorphous silicon layer (not doped) between doped amorphous silicon and crystalline silicon figure (II.6). This intrinsic layer is crucial to achieve high Vco values with HIT technology. Silicon heterojunction cells offer many advantages, including a significant potential to improve yield by optimizing amorphous silicon deposition for crystalline silicon passivation. In addition, the entire manufacturing process takes place at low temperatures (about $200^C$), which significantly reduces the thermal budget required.

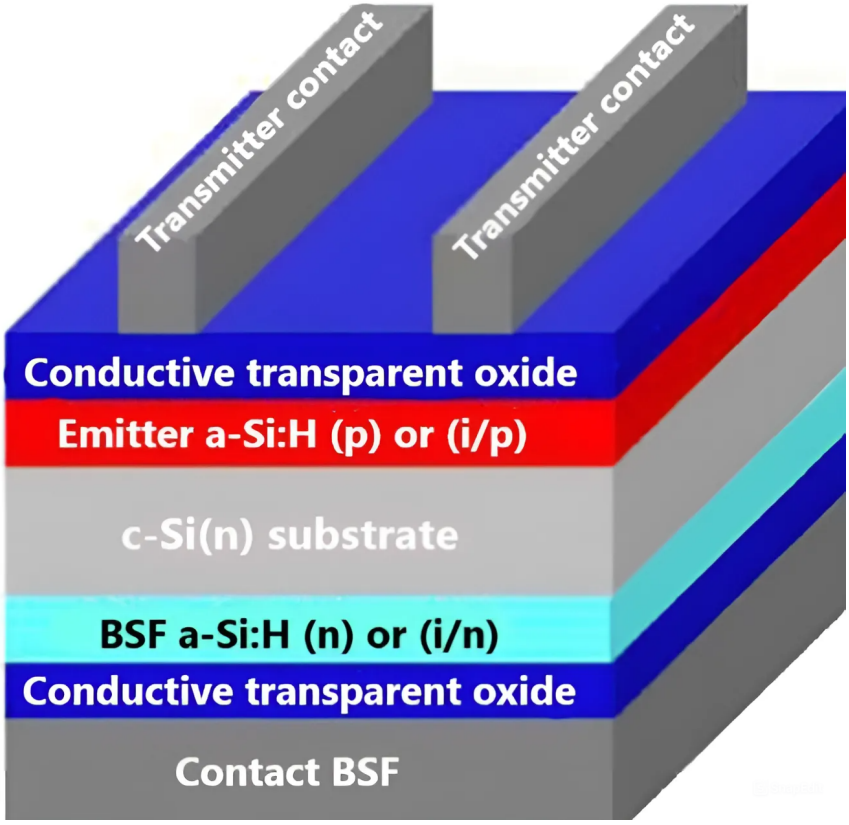


Figure II.6: Structure of a HIT cell.

The low temperature manufacturing process has several significant advantages for c-Si or mc-Si solar cells. On the one hand, it allows the use of thinner substrates, which reduces the risk of breakage and avoids potential degradation due to poor substrate quality. This reduction in substrate thickness is a preferred method to reduce the production costs of solar cells. Compared to silicon technology with homojunctions, which uses high temperature processes, the technology with heterojunctions is more suitable, especially because the thinness of the substrate accentuates the need for a good passivation of the surfaces. In addition, this technology is easy to implement and its transition to industrial scale is easy. Heterojunction silicon cells also offer better yield stability at different temperatures. Field tests have shown that the yield variation of these cells is less marked compared to homojunction cells, with degradation rates of $-0.33\%/°C$ versus $-0.45\%/°C$ for homojunction cells. Sanyo reported a 9% energy gain

for heterojunction cells with the same conversion efficiency as conventional cells. It is important to note that these gains may vary depending on the measurement conditions and type of sunshine, highlighting that these results are only one example of the improved capabilities of this technology.

# II Criteria for optimizing silicon heterojunction cells

To improve the manufacture of high-efficiency Si-HJ (heterojunction silicon) cells, it is essential to meet several optimization criteria:

- **Minimizing the density of interface states:**
  Meticulous surface cleaning is essential to avoid contamination before deposition of hydrogenated amorphous silicon (a-Si:H) layers. This helps to reduce defects that could impair the efficiency of the cell.
- **Adequate doping of a-Si:H:** The n and p-doped layers must be optimized to generate a robust electric field, while ensuring good electrical contact.
- **Insertion of a passivation layer:** In the presence of defective doped layers, it is crucial to introduce a buffer layer or "buffer" to reduce surface recombinations without impeding the conduction of the loads.
- **Strip Discontinuity Control:** It is necessary to find a balance between passivation (requiring a strong discontinuity) and conduction (favored by a low discontinuity) properties.
- **Compromise for OTC layers and metal electrodes:** These components must balance optical properties such as reflectivity, absorption and shading, with electrical properties such as conductivity. It is also important to note that the Staebler-Wronski effect, commonly observed in pi-n cells, does not affect the performance of Si-HJ cells. These maintain performance stability after exposure to light and actual operating temperatures .

# III Conclusion

This chapter explored the functioning and essential characteristics of heterojunctions in solar cells. The primary role of these heterojunctions is to minimize surface recombinations, thus reducing optical losses and resistance.

# Chapter III

# Simulation of a Heterojunction Photovoltaic Cell: a-Si:H(n)/a-Si:H(i)/c-Si(p)

# I Intoduction

The advancement of solar technologies increasingly relies on numerical simulation to understand and enhance the performance of solar cells. In this chapter, we will explore in detail the AFORS-HET numerical simulation software and the necessary steps to conduct accurate simulations. A thorough understanding of these aspects is essential for effectively utilizing the software in assessing the performance of heterojunction solar cells. We will go beyond merely introducing the software by also examining simulation results of the HIT a-Si:H(n) / a-Si:H(i) / c-Si(p) solar cell. This comprehensive analysis will enable us to determine the impact of geometric and physical parameters, such as layer thicknesses and acceptor and donor concentrations, on photovoltaic characteristics. We will particularly focus on key metrics such as short-circuit current density (Jsc), open-circuit voltage (Vco), fill factor (FF), and photovoltaic conversion efficiency. In summary, this chapter provides a deep dive into the use of AFORS-HET software for simulating and understanding heterojunction solar cells, thus offering valuable insights for the ongoing development of more efficient and high-performance solar technologies.

# II Presentation of the AFORS-HET simulation software

In this study, we focus on a comprehensive analysis of the electrical performance of Heterojunction with Intrinsic Thin layer solar cells using the AFORS-HET 2.5 simulation software (Automate FOR Simulation of HETerostructures). This software, developed in Germany by the Helmholtz-Zentrum Berlin (HZB) laboratory [20], is specifically designed to model and simulate silicon heterojunction solar cells. Heterojunction solar cells are distinguished by their multilayer structure, typically comprising layers of hydrogenated amorphous silicon (a-Si:H) and crystalline silicon (c-Si). This complex structure significantly enhances the efficiency of solar cells compared to conventional silicon cells by optimizing the collection and transport of charges across the various layers. Modeling the HIT solar cell in AFORS-HET is generally done in one dimension, meaning that the current flow is considered one-dimensional, following a specific direction through the cell. However, it is important to note that some innovative solar cells, due to their complex design or specific geometry, may require modeling in two or even three dimensions to more accurately account for current circulation and effects. By using AFORS-HET, we can thoroughly investigate the electrical performance of these heterojunction solar cells, analyzing parameters such as short-circuit current density (Jsc), open-circuit voltage (Voc), fill factor (FF), and photovoltaic conversion efficiency. This information is crucial for optimizing the design and performance of solar cells, thereby contributing to the development

of more efficient and sustainable solar technologies.

## II.1 Simulation Steps

The initial structure defined in AFORS-HET consists of the following layers:

- Front contact;
- Interface (MS-Schottky-Contact);
- Hydrogenated amorphous silicon layer (n-type) [a-Si:H (n)];
- Amorphous silicon layer [a-Si:H (i)];
- Crystalline silicon layer (p-type) [c-Si(p)];
- Interface (MS-Schottky-Contact); 7. Back contact

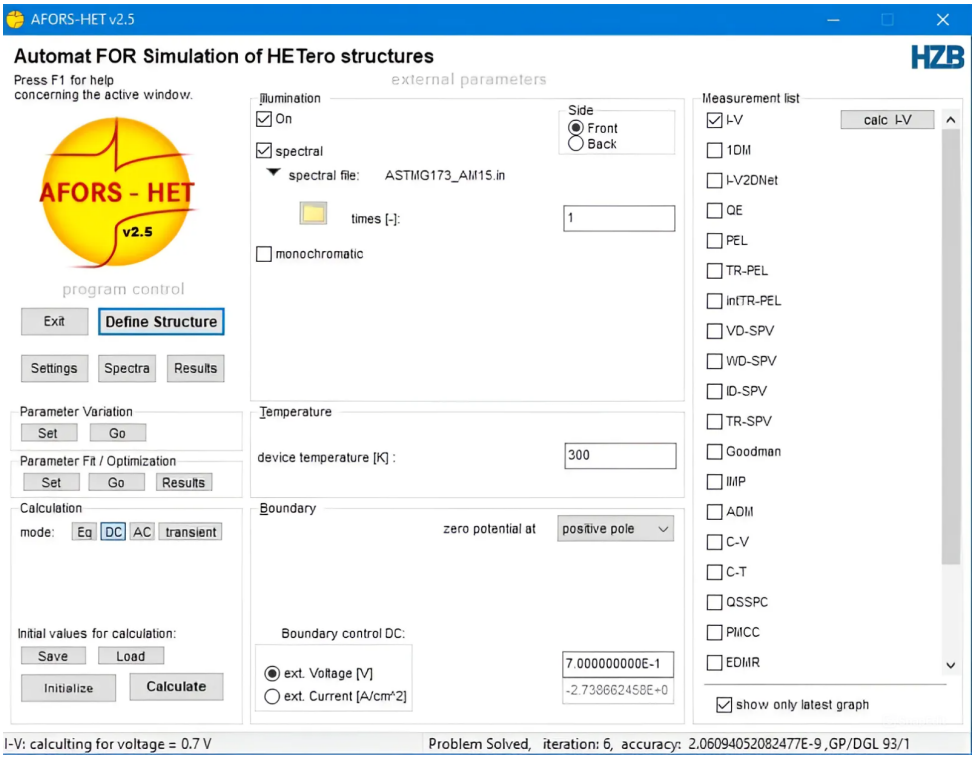


Figure III.1: Graphical Interface of AFORS-HET Software.

The interface of the AFORS-HET 2.5 software is illustrated in Figure (III.1) and consists of three distinct sections;[21]

- **Zone 1: Program control area**, where the user can define the structure to be simulated, the calculation mode, and the parameters to be adjusted.

- **Zone 2: External parameters**, which include parameters related to the simulation conditions of the cell such as temperature, boundary conditions, and solar spectrum.
- **Zone 3: Measurements**, where the user can select the measurements to be performed.

To start a simulation with this software, it is necessary to first define the structure of the cell to be simulated. To do this, you need to click on the "Define Structure" option. To add a layer, you must click on "add layer" to bring up the "layer" window. It is possible to overlay multiple layers with different parameters to construct a solar cell. It is also possible to introduce defects to model the quality of the layer. Once the structure is defined, the simulation can begin. This will bring up the window illustrated in Figure (III.2), [22]. The simulation of the (I-V) curve of a cell under illumination requires the activation of the direct current (DC) calculation mode. This method allows conducting calculations under nonequilibrium conditions, thus enabling the selection of constant external illumination as well as constant current or voltage values. Various options are available, including selecting different monochromatic or polychromatic lighting modes. In our simulation, we have chosen the direct current calculation mode with an AM 1.5G spectral illumination. This approach provides a precise perspective for studying the electrical behavior of the cell under different lighting conditions, which is crucial for understanding and optimizing photovoltaic figure(III.4), [22].

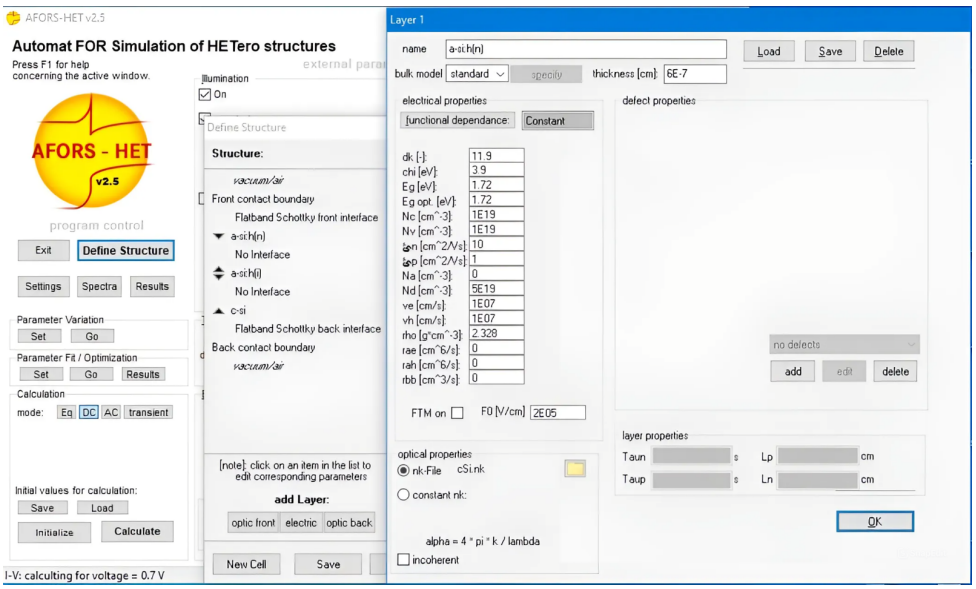


Figure III.2: Definition and parameter of the structure.

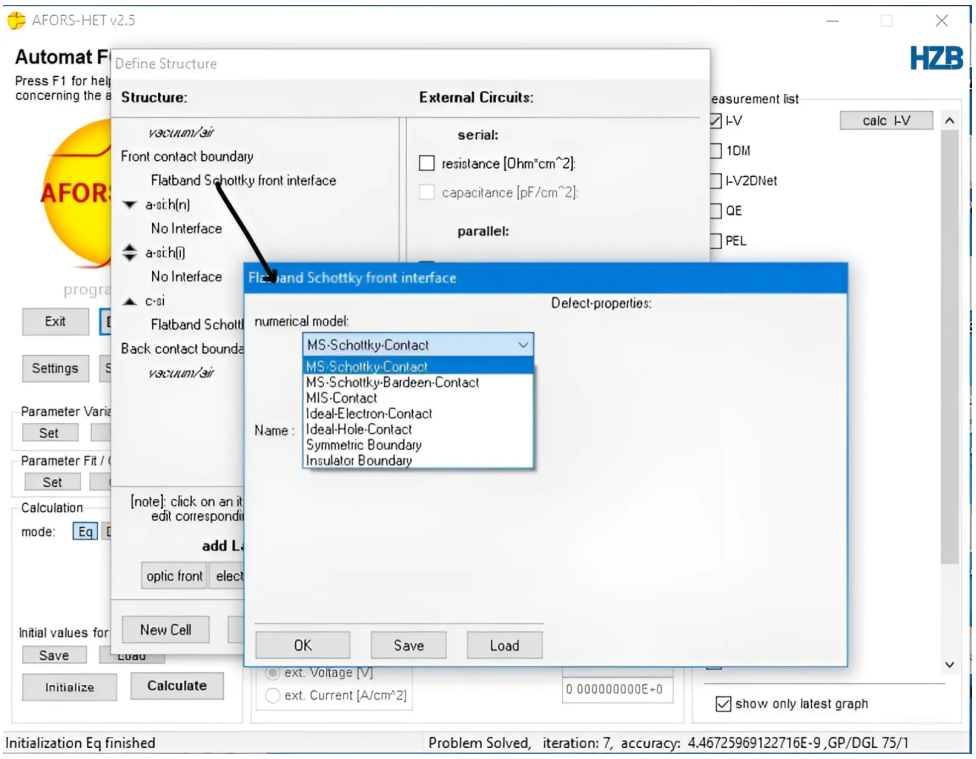


Figure III.3: Selection of the interface between two layers.

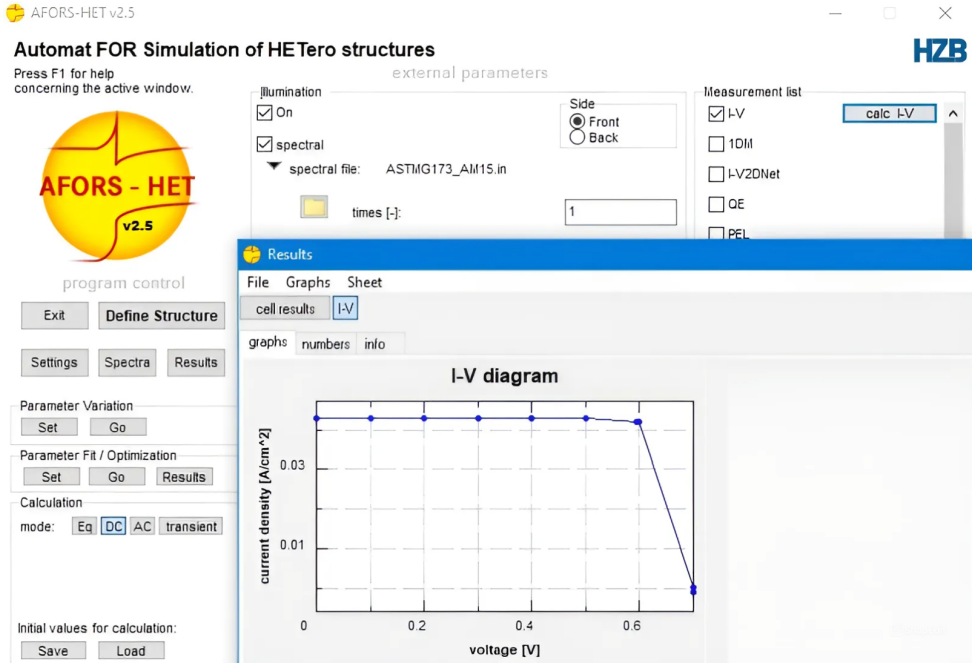


Figure III.4: (I-V) calculation of the cell under illumination.

# III Structure of the HIT Photovoltaic Cell

A solar cell is a device that converts solar energy into electrical energy through the photovoltaic effect. HIT solar cells are composed of an intrinsic layer of [a-Si:H(i)] placed between a doped layer of [a-Si:H(n)] and a doped layer of [c-Si(p)]. In this work, we examined HIT solar cells, as presented in Figure (III.4).

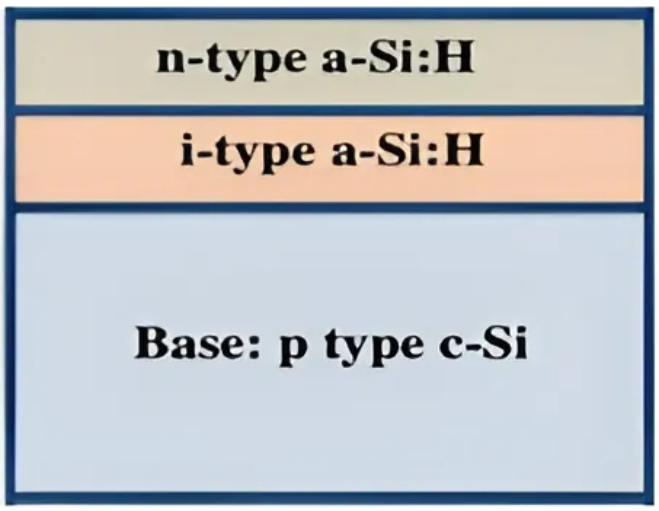


Figure III.5: Structure of the HIT Photovoltaic Cell.

# IV Parameters of the HIT Photovoltaic Cell

Table III.1: Different parameters for the layers of the HIT cell [20].

| **Parameters** | **a-Si:H(n )** | **a-Si:H(i)** | **c-Si(p)** |
|---|---|---|---|
| Thickness (nm) | (6-20) | (3-10) | $(10^5 - 3.10^5)$ |
| Relative permittivity, $\epsilon$r | 11.9 | 11.9 | 11.9 |
| Electron affinity, $\chi$(eV) | 3.9 | 3.9 | 4.05 |
| Energy gap, Eg (eV), fundamental parameter | 1.72 | 1.72 | 1.124 |
| Effective density of the conduction band ($cm^{-3}$) | $10^{19}$ | $10^{19}$ | $2.8.10^{19}$ |
| Effective density of the valence band ($cm^{-3}$) | $10^{19}$ | $10^{19}$ | $10^{19}$ |
| Electron mobility ($cm^2V^{-1}s^{-1}$) | 10 | 10 | 1040 |
| Hole mobility ($cm^2V^{-1}s^{-1}$) | 1 | 1 | 480 |
| Acceptor concentration ($cm^{-3}$) | 0 | 0 | $1.5.10^{16}(10^{16} - 7.10^{16})$ |
| Donor concentration ($cm^{-3}$) | $10^{19}(10^{17} - 10^{19})$ | 0 | 0 |
| Thermal velocity of electrons ($cms^{-1}$) | $10^7$ | $10^7$ | $10^7$ |
| Thermal velocity of holes ($cms^{-1}$) | $10^7$ | $10^7$ | $10^7$ |
| Layer density ($g/cm^3$) | 2.328 | 2.328 | 2.328 |
| Auger recombination coefficient for electrons ($cm^6s^{-1}$) | 0 | 0 | $2.2.10^{-31}$ |
| Auger recombination coefficient for holes ($cm^6s^{-1}$) | 0 | 0 | $5.10^{-32}$ |
| Band-to-band recombination coefficient ($cm^3s^{-1}$) | 0 | 0 | $9.5.10^{-15}$ |

# V Results and Discussions

## V.1 Influence of the thickness of the emitter layer a-Si:H(n)

In this section, we will expose the result of the simulation made to optimise the parameters of the studied structure. We will show in Figure (III.6) the effect of the thickness of the N-type a-Si:H emitter layer on the cell performance, showing the variation of Voc, Jsc, FF, and $\eta$ for the HIT cell.

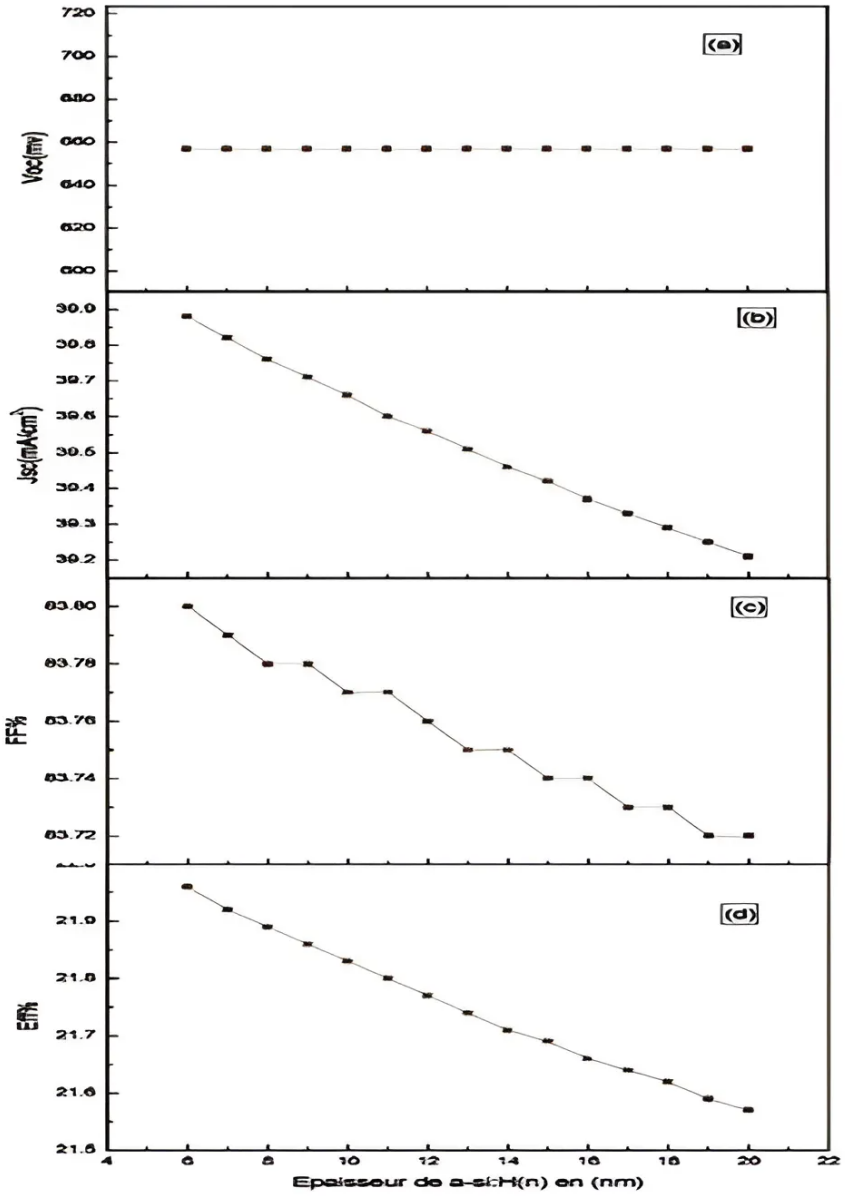


Figure III.6: Influence of the thickness of the a-Si:H(n) layer on the performance of the HIT cell.

We observe a decrease in cell performance with increasing thickness, where a decrease in Jsc from 39.88 $mA/cm^2$ to 39.21 $mA/cm^2$, $\eta$ from 21.96% to 21.57%, and FF from 83.8% to 83.72% is observed. For Voc, it remains constant at 657 V. The thickness of the emitting layer a-Si:H(n) in a Heterojunction with Intrinsic Thin layer cell has a significant impact on the cell's performance. As the thickness of this layer increases, there is a decrease in the cell's performance, primarily due to the low minority carrier (holes) diffusion length in the N layer (a-Si:H) compared to the minority carriers (electrons) in the P layer (c-Si). With an increase in the thickness of the emitting layer a-Si:H(n) , a large number of photons are absorbed in this N layer before reaching the P layer. This significantly reduces absorption in the P layer, where the conversion of light energy into electrical energy takes place. Consequently, a greater thickness of the emitting layer leads to a decrease in the efficiency of converting light into electricity, resulting in an overall decrease in cell performance. According to these results, the best performance is achieved with a thickness of 6 nm for the [a-Si:H(n)] layer.

### V.1.1 I-V Characteristic

The J-V characteristics of the HIT cell are calculated under standard conditions ($300°C$, AM1.5) and are depicted in Figure (III.7):

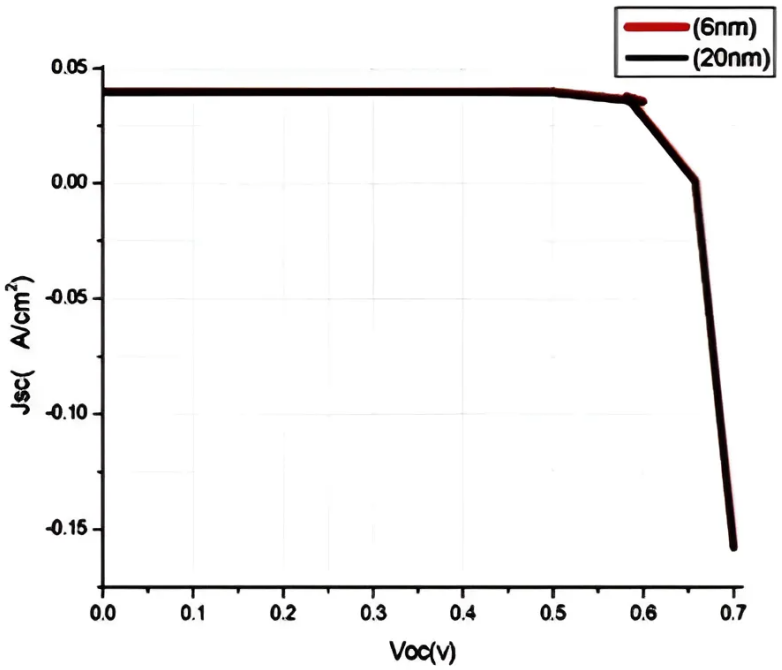


Figure III.7: J-V characteristic of the HIT cell for the two thickness values (6 nm and 20 nm).

The parameters Voc, Jsc, FF, and $\eta$ of the HIT amorphous cell for the two thickness values (high and low) of the [a-Si(n)] layer are summarized in the following table:

Table III.2: Performance of the HIT cell for the two thickness values of the a-Si:H(n) layer.

| (nm) | Voc(mv) | Jsc($mA/cm^2$) | FF% | Eff% |
|---|---|---|---|---|
| 6 | 657 | 39.88 | 83.8 | 21.96 |
| 20 | 657 | 39.21 | 83.72 | 21.57 |

## V.2 Influence of the thickness of the intrinsic amorphous silicon layer aSi:H(i)

In this section, we will present the influence of the change of the thickness layer of the intrinsic layer on the performance of the cell. The Figure (III.8) represents the effect of the intrinsic amorphous silicon layer a-Si:H(i) on cell performance, the variation of Voc, Jsc, FF, and $\eta$ for the HIT cell. We observe a decrease in cell performance with increasing thickness from 3 to 10 nm, where Jsc decreases from 39.92 $mA/cm^2$ to 39.81 $mA/cm^2$ and $\eta$ decreases from 21.98% to 21.91%. Voc remains constant at 657 V, while FF remains almost constant at 83.8%. This decrease is attributed to the low hole diffusion length in the [a-Si:H(i)] layer compared to the electron diffusion length in the [c-Si(p)] layer. This leads to an increase in photon absorption in the emitter layer [a-Si:H(i)], reducing absorption in the [c-Si(p)] layer. This explains the decrease in Jsc and $\eta$. These results indicate that the best performance is achieved with a thickness of 3 nm for the [a-Si:H(i)] layer.

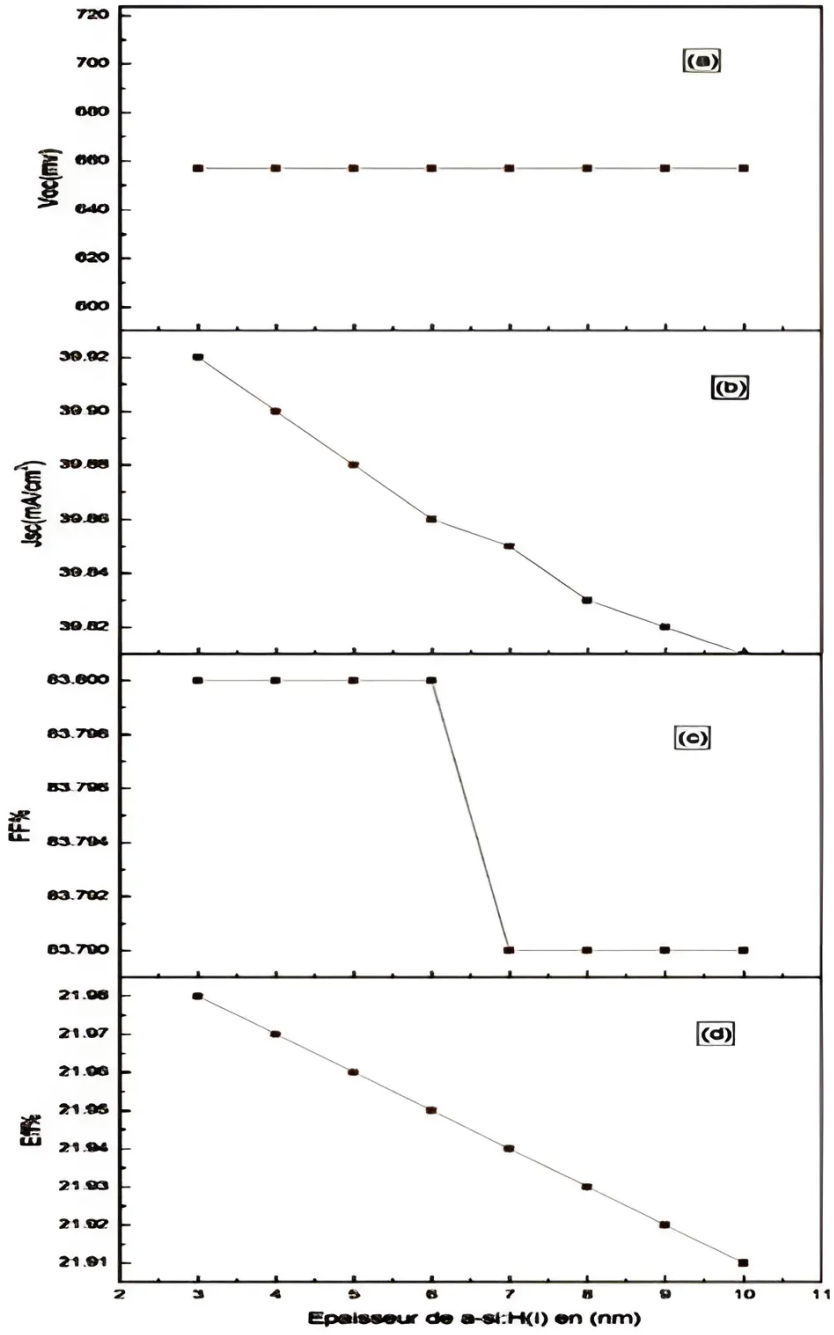


Figure III.8: Influence of the thickness of the a-Si:H(i) layer on the performance of the HIT cell.

### V.2.1 I-V Characteristic

The J-V characteristics of the HIT cell are calculated under standard conditions ( $300°C$, AM1.5) and are depicted in Figure (III.9):

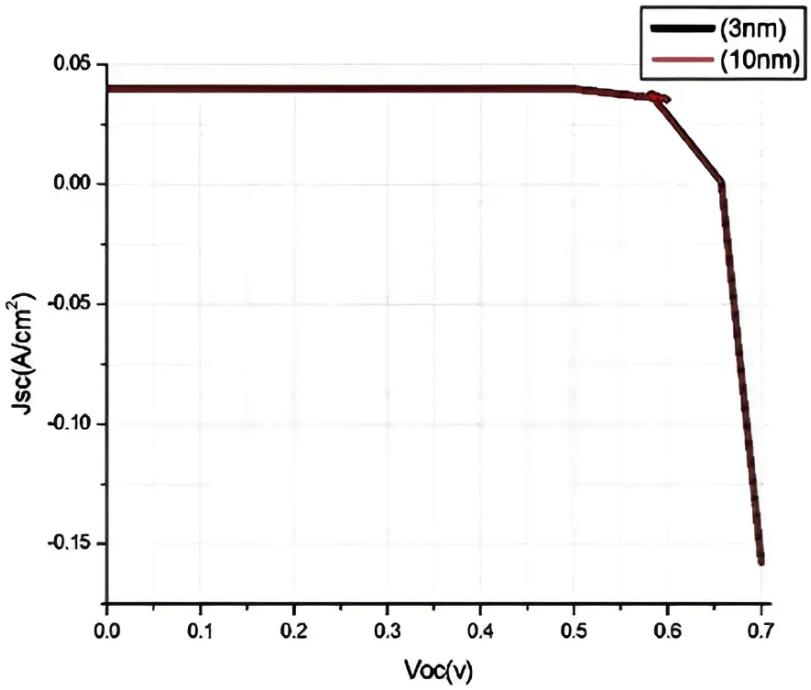


Figure III.9: J-V characteristics of the cell for the two thickness values of the a-Si:H(i) layer (3nm and 10 nm).

The parameters Voc, Jsc, FF, and $\eta$ of the HIT cell for the two thickness values (ideal and low) of the [a-Si(i)] layer are summarized in the following table:

Table III.3: Performance of the HIT cell for the two thickness values of the a-Si:H(i) layer.

| (nm) | Voc(mv) | Jsc($mA/cm^2$) | FF% | Eff% |
|---|---|---|---|---|
| 3 | 657 | 39.92 | 83.8 | 21.98 |
| 10 | 657 | 39.81 | 83.79 | 21.91 |

## V.3 Influence of the thickness of the absorber layer [c-Si(p)]

In this section, we will illustrate in Figure (III.10) the effect of the absorber layer [c-Si(p)] on the cell performance, showing the variation of Voc, Jsc, FF, and $\eta$ for the HIT cell:

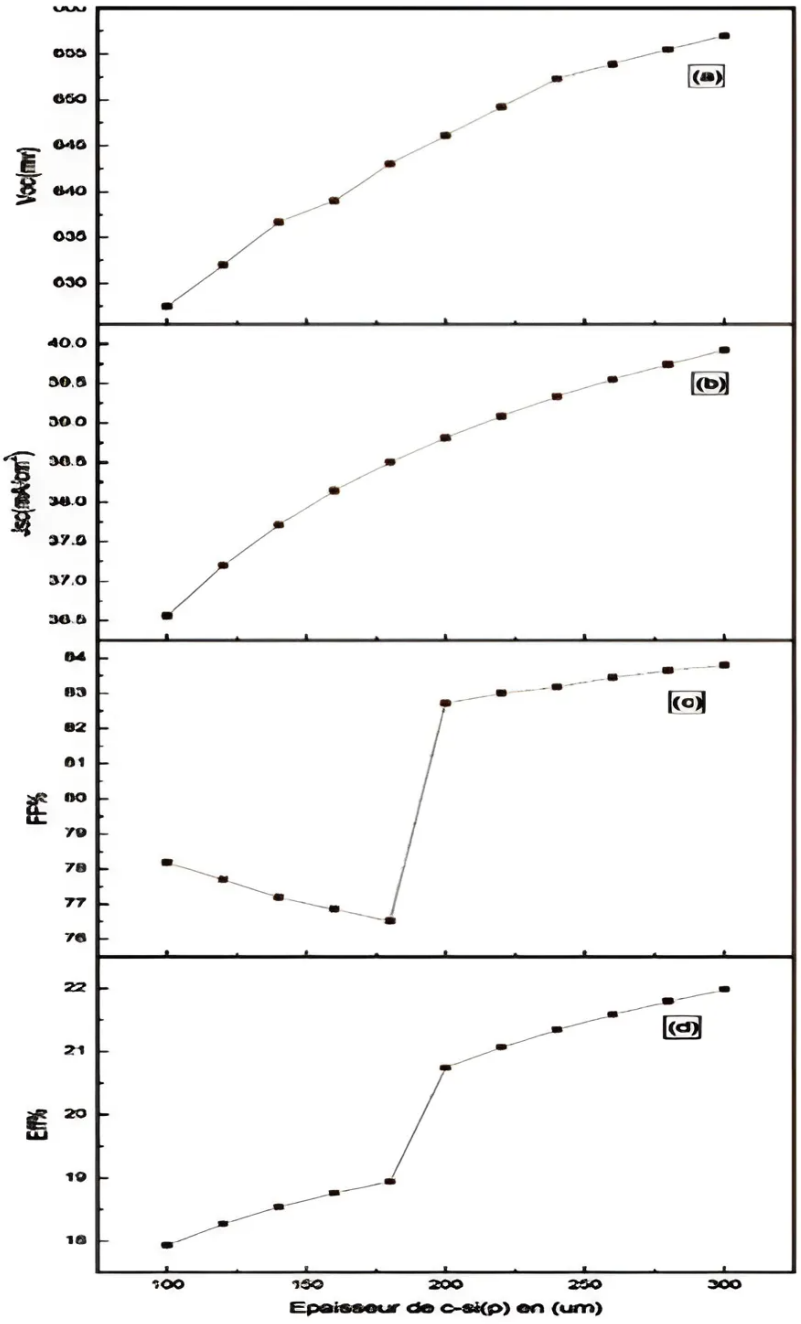


Figure III.10: Influence of the thickness of the c-Si(p) layer on the performance of the HIT cell.

We observe an improvement in cell performance with increasing thickness. Jsc increases from 36.52 $mA/cm^2$ to 39.92 $mA/cm^2$, Voc increases from 627.3 V to 657 V, and $\eta$ increases from 17.93% to 21.98%. As for FF, it initially decreases to 76.52%, then increases to reach 82.71% before finally reaching 83.8%. This improvement is related to the increase in absorp-

tion, leading to an increase in the number of generated electrons and holes. This explains the improvement in Jsc and $\eta$.

### V.3.1 I-V Characteristic

The J-V characteristics of the HIT cell are calculated under standard conditions ($300°C$, AM1.5) and are represented in Figure (III.11).

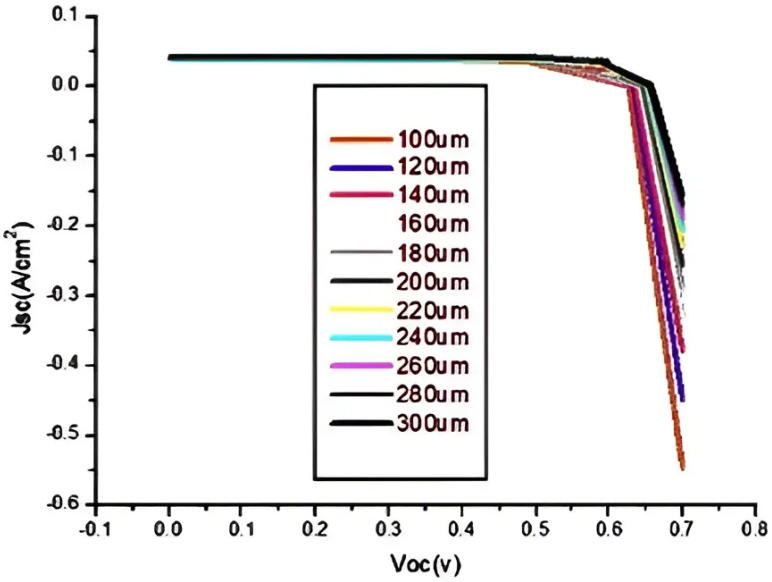


Figure III.11: J-V characteristics of the cell for different thickness values of the c-Si(p) layer (100 $\mu$m to 300 $\mu$m).

The parameters Voc, Jsc, FF, and $\eta$ of the HIT cell for the two thickness values (high and low) of the [c-Si(p)] layer are summarized in the following table:

Table III.4: Performance of the HIT cell for the two thickness values of the c-Si(p) layer.

| (um) | Voc(mv) | Jsc($mA/cm^2$) | FF% | Eff% |
|---|---|---|---|---|
| 100 | 627.3 | 36.56 | 78.19 | 17.93 |
| 300 | 657 | 39.92 | 83.8 | 21.98 |

## V.4 Influence of the doping of the emitter layer [a-Si:H(n)]

For this part, the simulation is conducted to study the influence of the doping concentration of the [a-Si:H(n)] on the performance of the HIT cell. The doping concentration Nd of the emitter layer is varied from $10^{17}$ to $5.10^{19} cm^{-3}$, as shown in Figure (III.12):

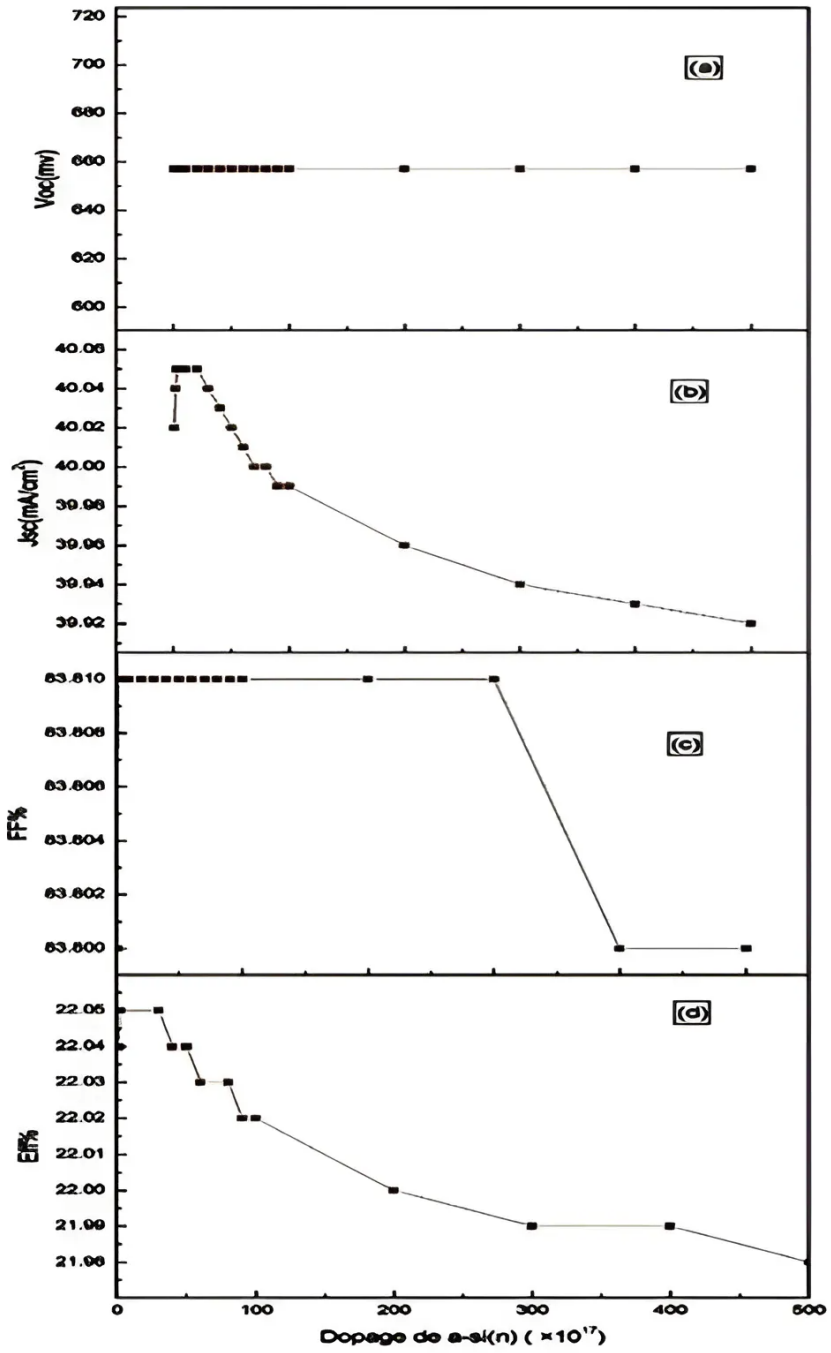


Figure III.12: Influence of the doping concentration of the a-Si:H(n) layer on the performance of the HIT cell.

We observe that $\eta$ and Jsc decrease slightly with the increase in $N_d$ ($\eta$ from 22.05% to 21.98% and Jsc from 40.02 to 39.92 ($mA/cm^2$)), while Voc remains constant and FF remains almost constant (Voc at 657 mV and FF nearly 83.81%). it appears that increasing the doping concentration (Nd) of the a-Si:H(n) layer leads to a slight decrease in both the efficiency ($\eta$) and the short-circuit current density (Jsc). However, the open-circuit voltage (Voc) remains constant, and the fill factor (FF) remains almost constant. This trend suggests that while higher doping concentrations may enhance carrier transport properties due to increased conductivity, they also lead to higher recombination rates, resulting in decreased efficiency and current density. Since Voc and FF remain relatively constant, it indicates that the change in doping concentration does not significantly affect the built-in potential and the internal series resistance of the solar cell. Therefore, the optimal performance, characterized by the highest efficiency, is achieved at a doping concentration of $3.10^{18}cm^{-3}$ for the a-Si:H(n) layer. This concentration likely strikes a balance between enhanced carrier transport and minimized recombination losses, resulting in the best overall performance for the HIT solar cell configuration .

## V.5 Influence of the absorber doping [c-Si(p)]

For this part, the simulation is conducted to study the influence of the doping concentration of the [c-Si(p)] on the performance of the HIT cell. The doping concentration Na of the emitter layer is varied from $10^{16}$ to $7.10^{16}$, as shown in Figure (III.13):

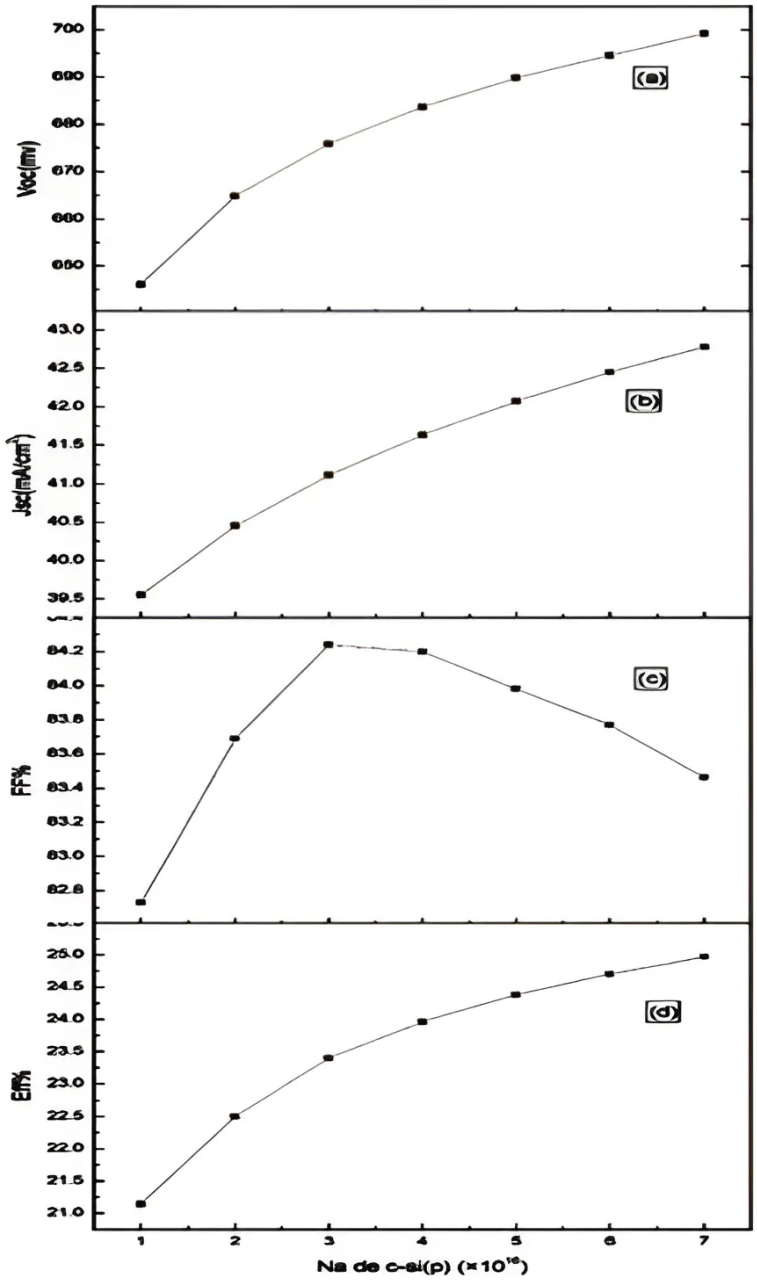


Figure III.13: Influence of the doping concentration of the c-Si(p) layer on the performance of the HIT cell.

We observe that $\eta$ and Jsc increase with the increase in Na ($\eta$ from 21.14% to 24.97% and Jsc from 39.55 $mA/cm^2$ to 42.78 $mA/cm^2$, and Voc from 646.1 mV to 699.2 mV), while FF increases with the increase in Na until $4.10^{16}$, then begins to decrease from 84.2% to 83.46%. The observed increase in efficiency ($\eta$) and current density (Jsc) of the HIT solar cell with increasing doping concentration (Na) in the c-Si(p) layer can be attributed to several factors. Higher doping concentrations enhance carrier transport properties by increasing the conductivity of the semiconductor material, leading to improved charge collection efficiency and higher current output. The increase in open-circuit voltage (Voc) further suggests reduced recombination losses and improved charge separation at the heterojunction interface. However, beyond a certain doping concentration threshold, the fill factor (FF) begins to decrease, indicating increased series resistance or recombination losses. The optimal performance achieved at a doping concentration of $7.10^{16}cm^{-3}$ suggests a balance between enhanced carrier transport and minimized losses, resulting in the highest overall efficiency for the HIT cell configuration.

# VI Conclusion

In the first part of this chapter, we presented and defined the AFORS-HET numerical simulation software. Then, we described the steps followed in the simulation and presented the structure of the HIT heterojunction solar cell a-Si:H(n) / a-Si:H(i) / c-Si(p), as well as the different parameters corresponding to each layer. In the second part of this chapter, we presented the simulation results for the HIT cell. The optimal structure of the HIT cell achieved a maximum efficiency of $\eta = 24.97\%$, with a Voc of 699.2 mV, a Jsc of 42.78 $mA/cm^2$, and an FF of 83.46%. The optimal parameter values are as follows: a thickness of a-Si:H(n) of 6 nm, a thickness of c-Si(p) of 300 $\mu$m, and a thickness of a-Si:H(i) of 3 nm, with $N_a = 7.10^{16}$ and $N_d = 3.10^{18}$.

# General Conclusion

This study focused on investigating the influence of parameters such as thickness and doping concentration of the various layers constituting a heterojunction photovoltaic solar cell: a-Si:H(n) / a-Si:H(i) / c-Si(p), on the cell's performance. The performance of the solar cells was evaluated in terms of open-circuit voltage (Voc), short-circuit current (Jsc), fill factor (FF), and conversion efficiency ($\eta$), through numerical simulations conducted using the AFORS-HET software. The results of this study demonstrate that: A reduced thickness of the emitter layer (a-Si:H(n)) enhances the efficiency, with an optimum at 6 nm. A greater thickness of the absorber layer (c-Si(p)) leads to higher efficiency, with an optimum at 300 µm. The maximum efficiency is achieved with the minimum thickness of the intrinsic layer (aSi:H(i)), with an optimum at 3 nm. The optimal performance, characterized by the highest efficiency, is achieved at a doping concentration of $3.10^{18} cm^{-3}$ for the a-Si:H(n) layer. The optimal performance of the absorber layer (c-Si(p)) is achieved at a doping concentration of $7.10^{16} cm^{-3}$. The optimal structure of the HIT cell achieved a maximum efficiency of 24.97% These findings highlight the importance of optimizing both the thickness and doping concentration of the various layers to maximize the efficiency of heterojunction photovoltaic solar cells. Finally, the structure of the heterojunction cell with buffer layer and with the following optimal parameters: $W_n = 6nm, W_i = 3nm, W_p = 300\mu m, N_a = 7.10^{16}$ and $N_d = 3.10^{18}$. gives the following best photovoltaic characteristics: $Jsc = 42.78 mA/cm^2; Vco = 699.2 mV; FF = 83.46\%$. and $\eta = 24.97\%$ In summary, this work underscores the critical role of precise parameter optimization, including both layer thickness and doping concentration, in enhancing the performance of heterojunction photovoltaic solar cells.

# Bibliography


[1] K.BENDJEBBAR,*Doctoral thesis Improvement of the efficiency of silicon photovoltaic cells* ,University of Science and Technology of Oran (Mohamed Boudiaf),2020.

[2] A.ARRAS,*End of study dissertation Characterization of photovoltaic cells based on aSi/c-Si silicon heterojunction*,ABOU-BEKR BELKAID UNIVERSITY-TLEMCEN ,2017.

[3] N.BELFIHADJ,*End of Study Project Memory Study and simulation of a p-type emitter for silicon heterojunction photovoltaic cells*, École Nationale Polytechnique ENP,2020.

[4] A.MECHERI,A.SANDALI,*End of study dissertation Simulation of a photovoltaic solar cell based on heterojunction: a-Si:H(n)/c-Si(p)*,KASDI MERBAH OUARGLA UNIVERSITY,2014.

[5] D.RACHED,*Doctoral theses Study and modeling of a HIT cell based on polymorphic silicon*,University of Science and Technology of Oran (Mohamed Boudiaf).

[6] T.Takahama, M. Taguchi, S. Kuroda, T. Matsuyama, M. Tanaka, S. Tsuda, S. Nakano and Y. Kuwano, *High Efficiency Single- and Polycrystalline Silicon Solar Cells Using ACJ-HIT Structure*, Procedings 11th European PVSEC, Montreux, Switzerland , 1057,1992.

[7] S. Taira., Y.Yoshimine, T. Baba, M. Taguchi, T. Kinoshita, H. Sakata, E. Maruyama and M. Tanaka, *Proceedings 22nd EU PVSEC*, Milan, Italy, 3-7 Sept, 932 2007.

[8] W. Fuhs, K. Niemann, and J. Stuke.*Heterojunctions of amorphous silicon and silicon single crystals*, Bull, Am, Phys, Soc, 19 :345–349 ,1974.

[9] H. Sakata, T. Nakai, T. Baba, M. Taguchi, S. Tsuge, K. Uchihashi, and Seiichi Kiyama,*20.7% Highest Efficiency Large Area (100.5 $cm^2$) HITTM Cell*, Proc, of the 28th IEEE PSC, pages 7–12 ,2000.

[10] Trends in photovoltaic applications,(1992-2005),*Technical report, IEA Photovoltaic Power Systems Programme*,September 2006.

[11] M. S. Shur, *GaN and related materials for high power applications*, in Symposium Proceedings of Material Research Society, Symposium E, Fall ,1997.

[12] *New Semiconductor Materials.Characteristics and Properties, Ioffe Institute*, St , Petersburg, Russie, http://www.ioffe.rssi.ru/SVA/NSM.

[13] Trends in photovoltaic applications 1992-2008, Technical report, *IEA Photovoltaic Power Systems Programme*, September 2009.

[14] Keck et al, *The Review of Scientific Instruments 25*, 331,1954.

[15] J. Czochralski, Z. Physik Chem. 92, 219,1918.

[16] M.F. Thorpe and D. Weaire, Phys. Rev. 26, 1581 ,1971.

[17] P.W. Anderson, Phys, Rev, 109, 1492 ,1958.

[18] J. Damon-Lacoste, *Vers une ingénierie de bandes des cellules solaires à hétérojonctions a-Si:H/c-Si. Rôle prépondérant de l'hydrogène* , thèse Ecole polytechnique, Palaiseau, 2007.

[19] W. Fuhs, K. Niemann, and J. Stuke, Bull, Am, Phys, Soc ,19, 345 1974.

[20] (s.d.). Retrieved from https://www.helmholtz-berlin.de/forschung/oe/se/siliziumphotovoltaik/projek
het/index-en.html .

[21] A. Mecheri, A. Sandali, *Simulation d'une cellule solaire photovoltaïque à base d'hétérojonction a-Si:H(n)/c-Si(p)*, Mémoire MASTER ACADEMIQUE, 2015.

[22] N. Belfihadj,*Étude et simulation d'un émetteur de type p pour les cellules photovoltaïques à hétérojonction en silicium*, INGÉNIEUR D'ÉTAT, École Nationale Polytechnique, 2020.

الجمهورية الجزائرية الديمقراطية الشعبية
République Algérienne Démocratique et Populaire
وزارة التعليم العالي والبحث العلمي
Ministère de l'Enseignement Supérieur Et de La Recherche Scientifique
جامعة غرداية

كلية العلوم والتكنولوجيا
قسم الآلية والكهر وميكانيك

Faculté des sciences et Technologies
Département d'automatique et d'électromécanique

Université de Ghardaïa

غرداية في : 26 نوفمبر 2024.

.....

# إذن بالطباعة (مذكرة ماستر)

بعد الاطلاع على التصحيحات المطلوبة على محتوى المذكرة المنجزة من طرف الطلبة التالية أسماؤهم:

1. الطالب (ة) : ..رياض بلحاج عيسى.....
2. الطالب (ة) : ..عبد الجليل باخضر.....
3. الطالب (ة) : .....

تخصص : .....طاقات متجددة في الكهروتقني.....

نمنح نحن الأستاذ (ة) :

| الاسم واللقب | الرتبة – الجامعة الأصلية | الصفة | الامضاء |
|---|---|---|---|
| محمد عزاوي | MCB جامعة غرداية | رئيس اللجنة | |
| بلعزاس سعيد | MCA جامعة غرداية | مصحح (1) | |
| | | مصحح (2) | |
| سبع الحاج يحيى | MCA-جامعة غرداية | مؤطر | |

الإذن بطباعة النسخة النهائية لمذكرة ماستر الموسومة بعنوان

Optimization of the parameters of a H.I.T heterojunction solar cell

إمضاء رئيس القسم

مساعد رئيس قسم الآلية والكهروميكانيك
مكلف بما بعد التدرج والبحث العلمي
حسن ناصر

جامعة غرداية
قسم الآلية والكهروميكانيك-2
كلية العلوم و التكنولوجيا

الممسوحة ضوئيا بـ CamScanner